

NASA-CR-3670 19830018977

NASA Contractor Report 3670

# A Study of the Stress Wave Factor Technique for the Characterization of Composite Materials

Edmund G. Henneke II, John C. Duke, Jr.,  
Wayne W. Stinchcomb, Anil Govada,  
and Alan Lemascón

GRANT NSG-3-172  
FEBRUARY 1983

RESEARCH COPY

FEB 1983

LANGLEY RESEARCH CENTER  
LIBRARY, NASA  
LANGFORD, VIRGINIA

**NASA**



NASA Contractor Report 3670

# A Study of the Stress Wave Factor Technique for the Characterization of Composite Materials

Edmund G. Henneke II, John C. Duke, Jr.,  
Wayne W. Stinchcomb, Anil Govada,  
and Alan Lemascon  
*Virginia Polytechnic Institute and State University  
Blacksburg, Virginia*

Prepared for  
Lewis Research Center  
under Grant NSG-3-172



National Aeronautics  
and Space Administration

**Scientific and Technical  
Information Branch**

1983

## TABLE OF CONTENTS

	Page
1.0 INTRODUCTION	1
2.0 REPRODUCIBILITY OF THE SWF MEASUREMENTS	3
2.1 Tests on Stabilization of System Instrumentation	3
2.2 Test Program for Optimizing SWF Measurement Technique	6
2.3 Tests for Determining Effect of Instrumentation Parameters	11
3.0 CORRELATION OF SWF WITH FAILURE LOCATION IN TENSILE SPECIMENS	16
4.0 INTERPRETATION OF SWF	20
5.0 CONCLUSIONS	25
6.0 REFERENCES	26

## 1.0 INTRODUCTION

Because advanced composite materials are finding ever increasing application in many different engineering structures, designers and users are interested in knowing as much about the properties and behavior of these materials as possible. One important area of study is nondestructive testing and evaluation of composites. A need exists for being able to detect damage and to predict remaining service based upon such detection. In addition, because these materials are relatively new, a need exists for nondestructive techniques which can monitor damage as it develops and yield information which can be used to develop failure theories applicable to composites. One such technique, which previous work by Vary and co-workers (Refs. 1-3) has shown to have potential in this respect, is the measurement of the Stress Wave Factor (SWF). A very important benefit of this technique is the fact that the measurement of the SWF yields a parameter which one might be able to use as a quantitative indicator of the mechanical quality of the material.

The work reported here covers the initial portion of a continuing investigation of the stress wave factor technique. This work was proposed to be an independent investigation and evaluation of the SWF technique for characterizing the mechanical behavior of glass epoxy composite laminates. The major objectives of this investigation were:

- (1) evaluate the reproducibility of the SWF technique;
- (2) obtain and evaluate relationships between microstructure, mechanical properties, and SWF;
- (3) compare the SWF technique with other NDE methods; and
- (4) correlate the SWF and other NDE data to sub-critical damage states caused by mechanical loading. The preliminary work covered by this

report period emphasized completion of objectives (1) and (2), but some work has been performed on objective (3) as well.

A major concern with any quantitative NDE technique is the reproducibility of the data. In particular, if one is to obtain a usable, meaningful parameter that is somehow indicative of expected material behavior, the obtained parameter must be reproducible from day-to-day, from operator-to-operator, and from specimen-to-specimen. To investigate the reproducibility of the SWF parameter, a large number of tests have been run on a single glass epoxy specimen. These tests included various couplants, methods of attachment, contact pressures, instrument settings, etc. These tests were performed until the operators became satisfied that they were able to obtain a reproducible value of SWF to within a 10% error. Details will be presented in the next section of this report.

After the test technique was refined to the point where the reproducibility of the data was within a  $\pm 10\%$  error, several tensile coupons of glass epoxy, composite material were prepared for measurement of SWF values along the length of the specimen. A significant number of tests were made, varying the parameters for SWF measurement and taking multiple readings for error analysis. These specimens were then tested in quasi-static tension to failure. Good correlation has been found between the point at which the specimens failed and the region having the lowest SWF values when a particular set of measurement parameters are chosen. Further details of these tests are given in section 3.0.

Section 4.0 of this report discusses a possible philosophy for interpretation of the SWF-material condition interrelationship. To support this idea, some preliminary results are given which show good

correlation between strain field measured by a moiré interferometric method and the SWF values. These results indicate that the stress wave factor appears also to measure some quality of the initial specimen which is related to local stiffness values of the material.

## 2.0 REPRODUCIBILITY OF THE SWF MEASUREMENTS

The initial portion of the work to be presented in this report involved measurement of the SWF by the AET Model 206 AU, Acoustic Emission/Stress Wave Analyzer (Acoustic Emission Technology Corporation). This device was designed specifically for the purpose of making measurements of the SWF but it also serves as a standard signal conditioner for normal acoustic emission monitoring. Using this device, an initial test program was designed to include three parts: i) the degree of stabilization of the test instrument, ii) techniques for measuring SWF and iii) reproducibility of the SWF measurement.

### 2.1 Tests on Stabilization of System Instrumentation

Early testing with the Model 206 AU led us to observe that two changes occurred in the instrument during the warm-up period. The first observation was that there was a noticeable change in the gate repetition rate with time. In particular, for a trigger rate of 1 kHz and a sweep rate of 312  $\mu$  sec/div, three and one-third gates were visible on the CRT at  $t=0$  (Fig. 1). After a warm-up time of four hours, four gates were observed on the CRT. It was not immediately apparent whether or not this gate shift had a large influence on the measured value of the SWF.

The second observation was that a decrease occurred in the level of the fixed threshold with time. As with standard acoustic emission

studies, the threshold level is a setting for counting excursions above a set level of the signal from the transducer. Each time the signal rises above this threshold level a single count is recorded. It was found that for our particular instrument a gradual decrease of 10-15% in the fixed threshold level occurred during the first four hours of warm-up of the instrument. After this time, the threshold level stabilized. Table 1 and Fig. 2 present the data obtained on three separate occasions for this shift.

The observation of such instrument changes is pointed out here as a cautionary advice for the experimenter and also because of the fact that such changes will affect any observations one might attempt to make concerning the reproducibility of the SWF measurement. One must obviously make sure that there are little or no instrumentation shifts if, over a long period of time, he is going to be making and comparing values of SWF from different parts of the same specimen or from different specimens.

In order to determine if there were any variations with time in the signal itself the signal was sampled at different times by a transient recorder and plotted. Figures 3 and 4 present typical results from one of five tests which were run in this manner. Figure 3 is an individual signal from a glass epoxy composite laminate acquired at a time after the instrument had warmed-up. The SWF at this time was 23,200. Twenty minutes later, the SWF had changed to a value of 20,800 (a 10.3% decrease) and an individual signal was again recorded (Fig. 4). Careful observation of the two signals shows that there is essentially no change in the signal itself. It thus appears likely that changes in measured values of SWF occur due to instrumentation

Table 1. Variation of the fixed threshold level (volts) versus time.

t=0	30 min.	60 min.	90 min.	120 min.	150 min.	180 min.	8 hr.	change	% change
2.00	1.91	1.85	1.81	1.79	---	---	---	0.21	11.0
2.00	1.90	1.87	1.85	1.84	---	---	1.79	0.21	11.1
1.00	0.93	0.91	0.89	0.88	0.87	0.87	0.85	0.15	16.1

variations and not due to any change in couplant or transducer which would directly alter the received signal.

## 2.2 Test Program for Optimizing SWF Measurement Technique

When making an SWF measurement, one must apply two transducers, a sender and a receiver, to the specimen. In making this connection, three parameters are important for consideration: i) the applied pressure between the transducer and specimen, ii) the type of coupling agent used between the transducer and specimen, and iii) the method of applying the transducers to the specimen (i.e., type of clamp, backing plate, etc.). Also, the instrument used to condition the signal and determine the stress wave factor may be adjusted in a number of ways, all of which may have some effect on the value of the SWF. Many different tests were run to obtain information in each of these areas. The important findings will be described in this section.

To obtain a constant reading of the SWF, it was found to be necessary to apply a load of at least two pounds on each transducer. As the applied load is increased, the value of the SWF decreases slightly, until, for loads of twenty pounds or more on each transducer, the value of SWF remains constant with load. For the larger values of load, however, one begins to notice some surface damage occurring on the specimen where contact is made with the transducers. As the SWF value was found to remain constant with load above twenty pounds, this value was selected for all subsequent tests since it caused no visible damage and is sufficiently high that one can easily reproduce its value from test to test without the danger of small variations in the load being responsible for variations in the measured value of SWF.

Several different types of couplants were tested once a fixed value of load applied to the transducer was selected. In the order of increasing viscosity, these couplants included Nonaq Stopcock grease, Ultrage1 couplant, Dow-Corning silicon grease, and Panametrics shear wave couplant. The largest viscosity couplant (Panametrics) provided the highest value of SWF for glass epoxy specimens when readings were taken at the same location on a given specimen under a fixed value of load applied to the transducers. Typical results are presented in Table 2. The maximum and minimum values reported for each run occur due to noise in the system. Between each run, the transducers were removed from the specimen, the surface was cleaned, and the couplant and transducers were reapplied. One might also note that Table 2 indicates that, for readings taken using Panametrics couplant, there is a smaller percentage difference in the noise variation for any run and a smaller standard deviation in the average values from run to run. Hence for all subsequent work reported herein, the Panametrics couplant was used.

As a further test on the effect of couplant upon the measured SWF value, three different methods for application of the couplant to the specimen and transducers were studied. The first method studied applied the couplant to both the transducers and the specimen with a spatula. This technique resulted in a relatively thick layer of couplant. The second method applied couplant to both surfaces with a razor blade, resulting in a thinner couplant layer. Finally, the third method was to apply couplant only to the transducers. There was no major effect on the measured SWF values as was expected, Table 3. In addition to these tests, a series of tests were made on a specimen before and after polishing the surface to remove the texture left by the scrim cloth

Table 2. Variation of SWF Values with four different coupling agents.

Couplant	Run Max	SWF (x100):			Auto Thres. Max	RMS (v)			
		Min	Avg	% Diff		Min	Avg	%	
Nonaq	1	132	124	128	6.5	.40	.38	.39	5.3
	2	174	162	168	7.4	.34	.33	.33	3.0
	3	144	132	138	9.1	.32	.31	.32	3.2
	4	162	142	152	14.1	.34	.34	.34	0
Avg. Stan. Dvi.	153 18.7	140 16.4							
Ultragel	1	132	116	124	13.8	.33	.32	.32	3.1
	2	176	152	164	15.8	.49	.47	.48	4.3
	3	92	92	92	0	.34	.32	.33	6.3
	Avg. Stan. Dev.	141 37.6	130 31.1						
Corning	1	194	184	189	5.4	.32	.30	.31	6.7
	2	180	172	176	4.7	.33	.32	.32	3.1
	3	170	138	154	23.2	.29	.27	.28	7.4
	4	122	116	119	5.2	.28	.27	.27	3.7
Avg. Stan. Dev.	167 31.3	153 31.2							
Panametrics	1	244	226	235	8.0	.42	.41	.41	2.4
	2	236	224	230	5.4	.43	.42	.42	2.4
	3	228	216	222	5.6	.39	.39	.39	0
	4	255	234	244	9.0	.43	.41	.42	4.9
Avg. Stan. Dev.	241 11.5	225 7.4							

Table 3. Results of study of various methods for applying couplant

Method	Number of Tests	SWF, Fixed Threshold	SWF, Auto Threshold Mean S.D.	RMS	
				Mean, S.D.	Mean S.D.
1	12	231 ± 23	165 ± 40	.34 ± .05	
2	5	251 ± 24	177 ± 18	.31 ± .07	
3	6	216 ± 24	144 ± 23	.36 ± .05	

during manufacture. There was a small difference in measured SWF values, but no significant improvement in the reproducibility of the measured SWF occurred.

The third parameter of importance for making the SWF measurement is the method of application of the transducers to the specimen. Several different fixtures and transducer arrangements were made and studied for the relative degree with which reproducible measurements could be obtained. Initially, the ability to obtain reproducible SWF values from the supplied transducer fixture was very poor because of the difficulty of applying a uniform load on each transducer when in the fixture. Figure 5 shows an arrangement which was found to work reasonably well. The transducers were each affixed to the specimen with a C-clamp which was tightened with a torque wrench so as to apply the load of 20 pounds to each transducer. A guide was made to maintain the center-to-center distance between the transducers. Several arrangements were tried for backing the sample. The best arrangement was determined to be that shown in Figure 5. A backing plate with two circular holes was placed immediately next to the specimen so that the holes were aligned directly under the transducers. A second plate was placed below the first one so that uniform pressure could be brought to bear on the entire arrangement. With this configuration, the reproducibility of measurement of SWF values was found to be within  $\pm 10\%$ . A later configuration was found to yield equally reproducible values but is much easier to apply. The transducers were remounted in the original fixture provided with the AET Model 206 AU. A spring tester, Fig. 6, is used to apply a fixed pressure to the fixture-specimen configuration. The specimen rests upon a plate which has two holes located directly below the posi-

tions of the transducers as is shown in Fig. 5. This arrangement, or a similar one which allows for the application of a steady, fixed pressure upon the transducers is recommended for reproducible measurements of the SWF.

### 2.3 Tests for Determining Effect of Instrumentation Parameters

In addition to the need for optimizing the experimental technique for attaching the transducers to the specimen, one must also determine the effect of the various parameters that can be set on the instrument, and hence determine if there are optimum conditions here as well. The SWF is characterized by a count rate made as for a standard acoustic emission test but performed on simulated waves. The simulated waves are generated by a transmitting ultrasonic transducer and are detected by a second, receiving transducer. After reception, the number of times the received signal rises above a fixed threshold is counted for a given time period. The actual value of SWF is then the total number of counts obtained in this time period. If the simulated waves are generated at repetition rate  $r$ , the number of times the signal rises above the threshold in each pulse or burst is  $N$ , and the counting period is  $g$  then the SWF is given by  $grN$ . These parameters are shown schematically in Fig. 7. Here each group of vertical lines represents a burst or pulse of simulated waves, the period  $P$  is the inverse of the repetition rate  $r$ , and  $T$  is the total time of counting. In this simple example, the SWF would be eighteen. When conditioning the signal to determine the SWF a number of parameters can be controlled. For the transmitter, one can set the repetition rate, the gain of the input signal to the transducer, the type of input (burst or pulse), and, if a burst signal is used, the frequency and duration. For the receiver, one can control

the amplification of the received signal. Finally, for the counting stage of the test, one can set the threshold level and the length of a time gate during which counts are made. As shown in Fig. 7, the gate is long enough to encompass one entire burst. However, one could shorten the gate so that not all six signal excursions above the threshold in each burst were counted.

The received signals are displayed upon a cathode ray tube in the Model 206 AU. As with most such displays, one can set the sweep time for the beam. Such a setting should affect only the display but not the SWF value. However, as shown in Table 4, some variation in SWF occurred when the sweep rate was changed, especially at the higher trigger rates. This may indicate a slight instability in the electronics for this particular instrument. Table 4 also indicates that, all other parameters remaining constant, the SWF varies directly proportional to the repetition rate of the simulated waves.

The next stage of our investigation was to determine what effect, if any, the various controllable parameters had on the reproducibility of the SWF. To perform these tests, the specimen surface was cleaned, couplant was applied and the transducers were applied to a precise location on the specimen. The SWF was measured with all parameters set and held constant. Readings of SWF were made utilizing the fixed threshold mode, and the automatic, or floating, threshold mode (which was designed to eliminate some of the effects of high background noise levels). Readings were also made of the RMS value for the received simulated waves. When one attempts to determine the SWF using the Model 206 AU, one finds that the value of SWF varies with time. A sufficient length of time was allowed to pass until the amount of variation noticeably

Table 4. Repetition rate of simulated waves versus sweep rate of CRT

	→ Sweep Rate, $\mu\text{sec}/\text{div}$							
	625	312	125	62.5	31.2	12.5	6.25	
2	286	286	286	270	269	286	285	
1	143	143	143	143	143	153	143	
.5	71	71	71	71	71	71	71	
.25	35	35	35	35	35	35	35	
2	648	648	634	614	632	695	675	
1	326	327	327	327	337	348	327	
.5	163	163	165	163	163	163	163	
.25	82	82	82	82	82	82	82	

decreased. At this point, high and low values of SWF (and RMS) were recorded for later averaging. The transducers were removed, the surface was cleaned, and the test was performed all over again. A minimum of six tests were performed for each set of parameters so that an average value and standard deviation could be obtained. One set of tests was performed on the glass epoxy specimen in the condition as removed from the press (normal surface condition) and a second set, in a condition where the surface was polished to remove the texture of the scrim cloth. The results of these tests are presented in Table 5. When measuring the SWF to determine the possible effects of the various instrumentation parameters on the reproducibility of its value, an attempt was made to vary them so that the SWF was of the order of two hundred. By doing this, one is able to compare more directly the mean and standard deviation of each measured value. Thus, in Table 5, when the repetition rate was doubled from 0.5 to 1.0, for example, the voltage applied to the transducer was reduced, yielding SWF numbers of  $160 \pm 13$  and  $144 \pm 23$  (fixed threshold), respectively. Otherwise, an increase of twice the repetition rate would cause an increase of twice the SWF number, as in Table 4.

Also, it should be noted that the gate width was set to either maximum or a certain number of graticule divisions on the CRT. It was later determined that the sweep on the CRT was not calibrated. Hence, the actual open time for the gate cannot now be specified.

Some general observations may be made after study of Table 5. For example, it appears that a repetition rate of 0.5 KHz provides a somewhat smaller standard deviation in SWF than the higher repetition rates. A more interesting observation may be made concerning the

Table 5. Results of reproducibility tests at various instrument settings

Normal Specimen Surface									
No. of Tests	Input Gain dB	Repetition Rate KHz	Pulser Gain	Threshold	Gate**	Sweep $\mu$ sec div	Automatic SWF	Fixed SWF	RMS
6	65	.5	1	0.25	open	62.5	182 $\pm$ 10	227 $\pm$ 9	.72 $\pm$ .01
6	65	.5	1	1.00	5 div	62.5	166 $\pm$ 8	187 $\pm$ 7	.68 $\pm$ .05
6	65	.5	1	2.00	open	62.5	116 $\pm$ 9	137 $\pm$ 4	.70 $\pm$ .05
12	65	1.0	3	1.00	open	312	231 $\pm$ 23	174 $\pm$ 18	.33 $\pm$ .03

Polished Specimen Surface									
No. of Tests	Input Gain dB	Repetition Rate KHz	Pulser Gain	Threshold	Gate**	Sweep $\mu$ sec div	Automatic SWF	Fixed SWF	RMS
6	75	.5	3	1.00	open	312	194 $\pm$ 4	154 $\pm$ 10	.55 $\pm$ .08
6	75	.5	3	1.00	4 div	3.2	159 $\pm$ 12	180 $\pm$ 15	.51 $\pm$ .04
6	65	.5	1	1.00	open	62.5	159 $\pm$ 23	200 $\pm$ 19	.58 $\pm$ .04
12	65	.5	1	1.00	5 div	625	193 $\pm$ 7	160 $\pm$ 13	.58 $\pm$ .04
6	65	1.0	3	1.00	open	3.2	215 $\pm$ 24	144 $\pm$ 23	.36 $\pm$ .05
6	60	1.0	1	1.00	open	625	225 $\pm$ 22	323 $\pm$ 39	.74 $\pm$ .03
6	60	2.0	3	1.00	open	312	183 $\pm$ 35	109 $\pm$ 21	.33 $\pm$ .06
6	60	2.0	3	1.00	open	625	121 $\pm$ 13	257 $\pm$ 60	.40 $\pm$ .04

\*Voltage to pulser 1:(-250v), 3:(-50v)

\*\*Sweep was not calibrated

threshold level and the gate width. The smaller standard deviations are generally obtained with higher threshold levels and smaller gate widths. The reason for this smaller variability is shown schematically in Fig. 8. If the threshold level is set low, the counter will begin to detect some of the noise at the tail end of the signal. This noise will be somewhat random in comparison with the actual simulated signal. Similarly, if the gate is set to its wider levels it will also allow the counter to detect some of the higher level noise at the end of the signal. There is, however, a trade-off that must be made. If the threshold is set too high and the gate width too short, then it is possible that a situation might exist where the same SWF value is obtained for two distinctly different signals as shown in Fig. 9. Hence, in order to obtain meaningful values of SWF, one should first be careful to observe the shape of the simulated signal and choose instrumentation parameters accordingly. In general, we found that use of the automatic threshold (which eliminates some of the noise from the counting circuits), an intermediate threshold setting of 1.00 v and an intermediate gate width setting allows one to obtain reproducible SWF values to within  $\pm 10\%$ .

### 3.0 CORRELATION OF SWF WITH FAILURE LOCATION IN TENSILE SPECIMENS

A very extensive testing program was next undertaken to study the correlation of the SWF value with mechanical properties of E-glass epoxy composite laminates. A large number of measurements were made on several different specimens. In general, the outcome of these experiments showed that a very probable correlation exists between initial SWF number and the location of the final failure site in the laminates when tested in quasistatic tension. However, to detect this correlation, one

needs to exercise extreme care when selecting the appropriate instrumentation parameters for conditioning and counting the signals of the simulated waves. This section will be written chronologically to present the data in the same fashion it was observed in the laboratory.

The E-glass epoxy specimens used in this study were nominally either two inches or one inch wide by eight inches long. Several different stacking sequences were investigated. For each specimen, initial measurements were made of the SWF before the specimen was loaded quasi-statically to failure. The SWF was measured at eight different positions along the longitudinal axis and at eight different positions transverse to the axis (for the wider specimens only), Fig. 10. The transducers were mounted in the AET fixture which maintained a distance of 1 1/2 inches between transducer centers. In Fig. 10, the transducers were placed so that their centers were located at the ends of each position when the longitudinal measurements were made. Hence there is some overlapping of material covered by consecutive measurements. For the transverse SWF measurements, the line joining the transducer centers was perpendicular to the specimen axis.

At each specimen position, ten individual measurements of SWF were made for fixed values of the following parameters: threshold levels, gate width, fixed threshold, and automatic threshold. Table 6 summarizes the tests that were run. For each SWF measurement, the transducers were removed from the specimen, the couplant was cleaned from the surface, and the test procedure was repeated as originally with the transducers being applied to the same position on the specimen for a total of ten times at each location.

Table 6. Summary of experimental conditions

Threshold Level	Number of Tests Per Point					
	Longitudinal Positions			Transverse Positions		
	Fixed SWF	Auto SWF	RMS	Fixed SWF	Auto SWF	RMS
0.25v	10	10	10	10	10	10
0.50	10	10	-	10	10	-
1.00	10	10	-	10	10	-
1.50	10	10	-	10	10	-
2.00	10	10	-	10	10	-
2.50	10	10	-	10	10	-
3.00	-	-	-	10	10	-
3.50	10	10	-	10	10	-
4.50	10	10	-	-	-	-

Note: This table was repeated for two gate widths: open and four divisions.

For the resulting data, two types of data presentations were developed. First, the values of SWF were graphed versus the threshold level. An example is given in Fig. 11. The shape of all the other graphs, i.e., for the other positions and gate widths, were very similar to that shown in Fig. 11. The error bars, as indicated in Fig. 11, were generally smaller for the lower threshold levels.

A second method for presenting the data is to graph the values of (longitudinal) SWF against position along the specimen, keeping all other parameters constant. An example of this is shown in Fig. 12. Here the SWF value obtained by the automatic threshold feature is plotted versus the longitudinal position along the specimen. The gate width was set to four divisions on the CRT and each of the four broken lines in Fig. 12 corresponds to a different value of threshold level. The most immediately apparent fact from such data is that the SWF value is highly dependent upon the instrument setting. If one were to attempt to use such raw data to predict, for example, the ultimate failure location in the specimen, it would be quite hazardous to do so. The 1.0 volt threshold level would indicate, based upon the lowest value of SWF, that the failure location would be approximately at position 12. On the other hand, if a threshold level of 1.5 v were used, the failure would be predicted to occur around position 18, while a threshold level of 0.5 v would predict the position 15 or 19. It should be pointed out here that one might also plot the transverse SWF values as a function of position along the specimen. When this was done, it was found that there was no correlation, in general, between the predictions of transverse and longitudinal SWF values. That is, the low values of

transverse SWF did not generally occur at the same region as the low values of longitudinal SWF.

This specimen, ( $[0,90_3]_S$ , E-glass epoxy laminate) was then loaded quasistatically to failure. The final failure location is indicated by the shaded area at the bottom of Fig. 13. At this point, each member of the various curves that had been plotted as in Fig. 12 were checked to determine, after the fact, which set of parameters would have come most close to predicting the final failure location. As indicated in Fig. 13, the one member of the family which most closely predicted failure was that one having the following set of parameter values: threshold level: 1.00 v, automatic threshold, gate width: four divisions, longitudinal SWF. An additional four specimens were tested using exactly the same experimental testing regime. After each failure, the single member of the family of SWF - position curves which most closely predicted the final failure site was found to have exactly the same set of parameters given above, Figs. 14-17. Thus, it appears at this time that the SWF correlates well with final failure location if the material - SWF measurement system is carefully calibrated.

#### 4.0 INTERPRETATION OF SWF

The question of how to interpret the effect a material has on a mechanical wave propagating through it is, to say the least, a classical one. In general, consideration must be given to reflections, mode conversions, various attenuation mechanisms, dispersion, etc. Any variation in material condition will normally cause a change in one or more of the areas mentioned. A precise description of a material's condition is, however, not possible using these concepts. It must be

recognized, of course, that a precise description of the material's condition will at best facilitate a determination of the stiffness since the strength or life depend on the nature and history of the applied loads. In a large structure, the task of determining the condition of the material everywhere is impractical so it is much more desirable to determine where the condition is poor. Knowing this, attention can then be directed at ascertaining the exact condition. It would appear that the SWF technique as applied in this study possesses a tremendous potential for doing just this type of inspection. Experimental evidence indicates that a low stress wave factor corresponds to a region in which the mechanical response is poor, relatively speaking. "Why is this so?" is a question which comes to mind immediately. "Can the SWF value obtained at fixed settings be uniquely related to the material's condition?" is another. Several findings of this study seem to provide insight regarding these questions.

First, since the SWF procedure utilizes two transducers in contact with the same side of the specimen, a technique performance parameter exists which is arbitrary, i.e., transducer separation. While a minimum value may be selected based on the reality of the finite transducer size, a maximum value of the separation is less obvious. Furthermore, since at least the volume of material between the transducers influences the measurement, some confusion exists as to how to associate the SWF value with the material being examined so as to allow for meaningful data interpretation. This dilemma is shown graphically in Fig. 18 for a region of material which is three times as long as the transducer separation and where the examination is performed without any overlap of the regions being examined. Any attempt to localize the measurement to a

point causes an artificial shifting of the data. That is, in Fig. a) the value of SWF has been designated as being the value for the entire region between the transducers. In Fig. b) the SWF value has been assigned to the point where the transmitting transducer was placed, while in Fig. c), it has been assigned to the location of the receiver. If the regions of inspection overlap, localization of the values to a point still causes data shifting, but eliminates the confusion of more than one SWF value at the same location, Fig. 19. In this instance, however, the assignment of an SWF to the transmitter, Fig. b) or to the receiver, Fig. c), will cause a relatively large misplacement of the predicted failure location, i.e., the point of lowest SWF. An alternative procedure which enables an association of the SWF value with a local region of the material has been devised. It involves averaging in conjunction with the overlap measurement procedure. This is described pictorially in Fig. 20 and has been applied to the data used to obtain the plot in Fig. 13 and then yields Fig. 21.

It is interesting to note that if one limits the spacing between transducers by the special case of the same transducer acting as both sender and receiver one realizes that the measurement of SWF would be related to the conventional pulse-echo A-scan. However, the unique feature of the SWF technique is the sensitivity of the technique to the structural configuration of the object. That is to say that the material's internal structure, ply interfaces, ply orientation, and boundaries cause the stress wave to propagate out into the specimen to a point where the receiver is located. This feature makes it possible in thin specimens to interrogate the material in the same directions in which stresses resulting from applied load would act. Interrogation in

these directions, as such, would be expected to find regions of the material responding in a fashion which would be peculiar to their condition, as related to mechanical performance. For example, the region which has a poor performance regarding stress wave energy propagation would be expected to test as a region of low SWF. If this number is the lowest in the object, its performance would be considered to be the poorest. Consequently, if all the regions were subject to an identical state of stress, the deformation in this region might be expected to be the most severe, and the site at which failure initiates. As has been indicated earlier, clear evidence exists which supports this suggestion.

However, some question exists regarding the exact relationship of the measured SWF and the strength. Further, because of the terminal nature of strength determining tests, the potential strength of other regions cannot be determined. It is important to recognize at this point in addition that the strength is dependent on the applied load history and future. That is to say, for a particular piece of material, the strength of any region is not unique. Consequently it is questionable to expect a relationship to exist in general between the SWF measure and strength. One may expect a particular relation to exist between SWF, strength, and specific load history. On the other hand the stiffness of the material is dependent on its present condition alone. Therefore the likelihood of some correlation existing between stiffness and SWF is plausible.

As is perhaps already evident, the term "stiffness" is being used in a somewhat unorthodox fashion. Classsically, stiffness is considered to be a structure-insensitive property. However, because the very

nature of the composite material is that of a structure, the property of stiffness must of necessity be structure sensitive. This is not to say that the stiffness of the constituents of the composite material, i.e., the fiber and the matrix is structure sensitive. Nevertheless it is necessary to recognize that, since laminated composite materials may in general continue to support load even after sustaining considerable damage and may exhibit property variations from point to point in even the undamaged condition because of problems during manufacture, determination of stiffness is inextricably linked with a gage length.

As part of the work conducted under this grant several experiments were performed which were directed at comparing the stiffness of the material to the measured SWF. The technique of moiré interferometry was utilized to obtain whole field in-plane displacements during quasistatic tension (Appendix). Since the interference patterns obtained may be interpreted as displacement, it is possible to determine the stiffness at every point along the length of a straight sided coupon specimen, subjected to tensile load. Fig. 22 shows the moiré interferometric pattern obtained for 2000  $\mu$ strain applied to a 1 inch wide  $[0,90_3]_5$  E-glass epoxy laminated specimen. Using this pattern, the local stiffness was determined along the length of the specimen. These results have been compared with SWF measurements made on the same specimen, Fig. 23. Close correlation can be seen for this example in which the averaging scheme described earlier has been used. Further work is necessary regarding this correlation in that a variety of material conditions may give rise to the same material stiffness. This is because the stiffness integrates all of these individual effects. Now although the SWF measurement also integrates, it has not been

established that there exists a one to one correlation between SWF and stiffness. That is, different material conditions which give rise to the same stiffness may be measured as being different by SWF, or vice versa.

## 5.0 CONCLUSIONS

An extensive, careful testing program has been performed to determine the reproducibility of measurement of the stress wave factor. Many different parameters were varied, including couplant, load between transducers and specimen, backing arrangement, surface condition, and instrumentation settings. Using the AET Model 206 AU, it was found that all of these parameters played some role in affecting the absolute value and standard deviation of the SWF. The standard deviation can be reduced by optimum selection of particular values of these parameters. After many tests and observations, it was determined that the SWF value can be measured reproducibly to within an error of  $\pm 10\%$  if care and experienced operators are used.

Further tests were performed to investigate the correlation between local SWF values along the length of E-glass epoxy laminates and the site of final, catastrophic failure when tensile loading was applied. It was first found that the SWF versus position curves will vary substantially depending upon one's choice of instrumentation parameters used to make the SWF measurement. A different set of parameters will yield a different location of the lowest SWF value. If one wishes to relate the lowest value of SWF with final failure site, it is mandatory to perform a careful testing and calibration program, using a wide range of parameter settings. We found that, after testing three coupons, there was one member of the family of SWF-position curves which

correlated most closely with the final failure site. For each specimen, this particular member had precisely the same instrumentation parameters in each case. Additional tested specimens were investigated using the same parameters for SWF measurement to predict a priori the final failure site. In each case, the prediction was closely verified.

A moiré interferometry technique, applied to two E-glass epoxy specimens, was used to determine the in-plane displacements during application of a tensile load. The local strain fields, i.e. the displacement gradients, were found to be inhomogeneous because of local differences in material stiffness. When SWF measurements were compared with the strain field, it was found that close correlation existed between those regions when the strain was the greatest (or local stiffness the least) and the region of material having the lowest value of SWF. Whether or not this observation will hold in general has yet to be determined.

#### 6.0 REFERENCES

1. Vary, A. and Bowles, K. J., "Ultrasonic Evaluation of the Strength of Unidirectional Graphite-Polyimide Composites," NASA Technical Memorandum, NASA TM X-73646, Apr. 1977.
2. Vary, A. and Bowles, K. J., "Use of an Ultrasonic-Acoustic Technique for Nondestructive Evaluation of Fiber Composite Strength," NASA Technical Memorandum, NASA TM-73813, Feb. 1978.
3. Vary, A. and Lark, R. F., "Correlation of Fiber Composite Tensile Strength with the Ultrasonic Stress Wave Factor," NASA Technical Memorandum, NASA TM-78846, Apr. 1978.

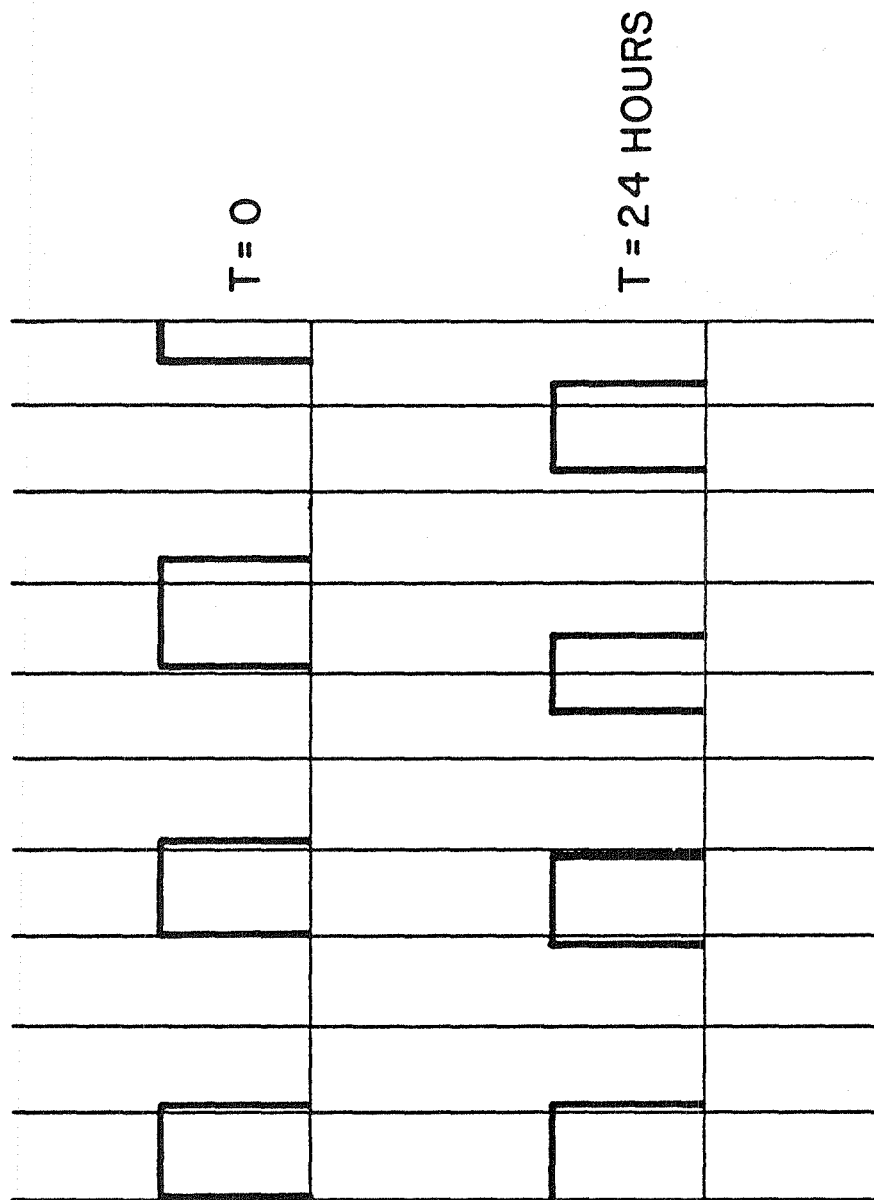


Figure 1. Observed time variation of gate repetition rate during warm-up.

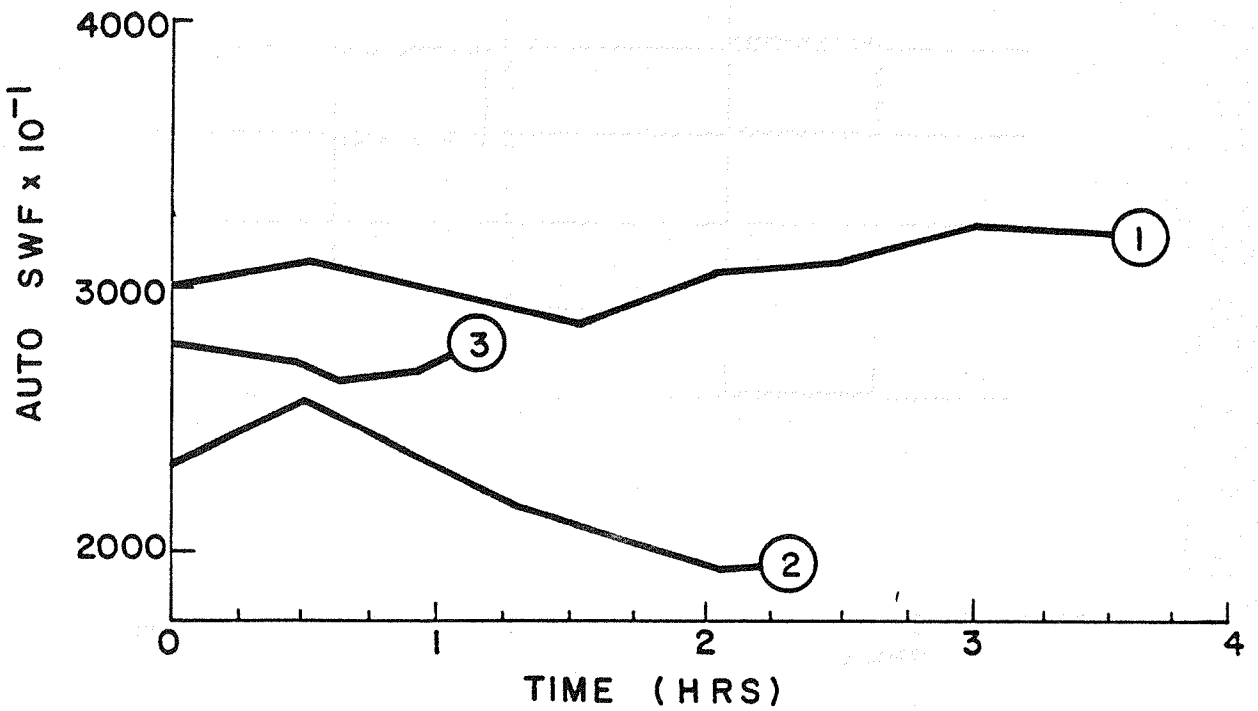
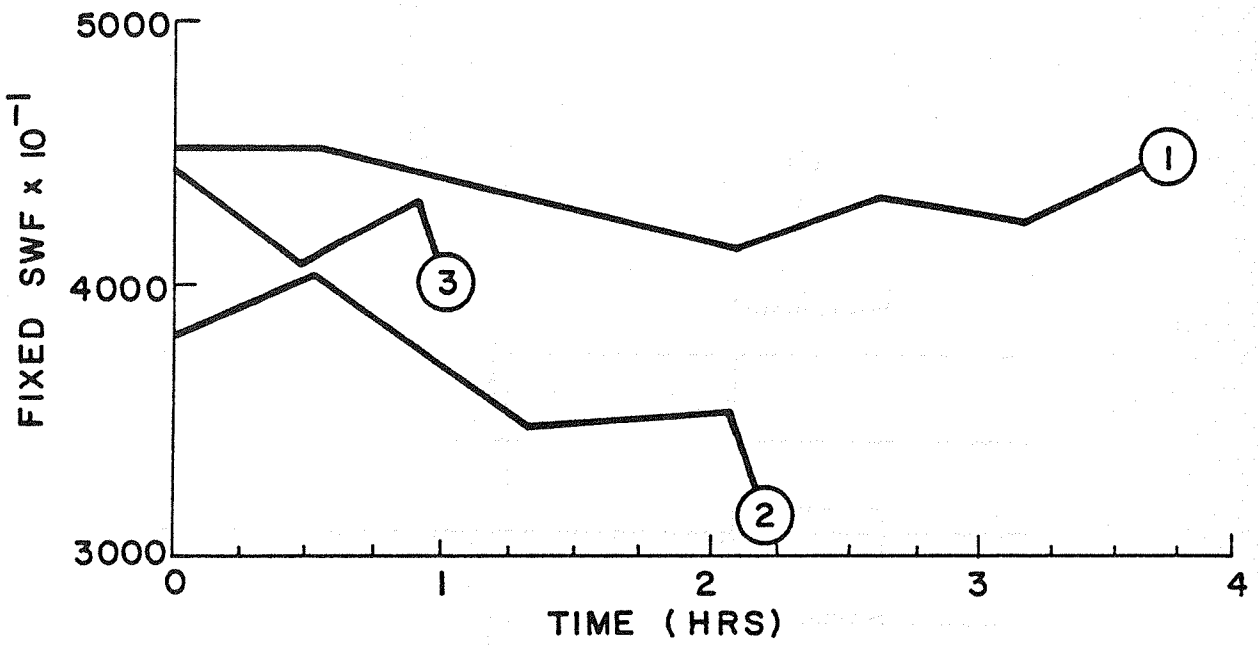


Figure 2. Variation of SWF with time.

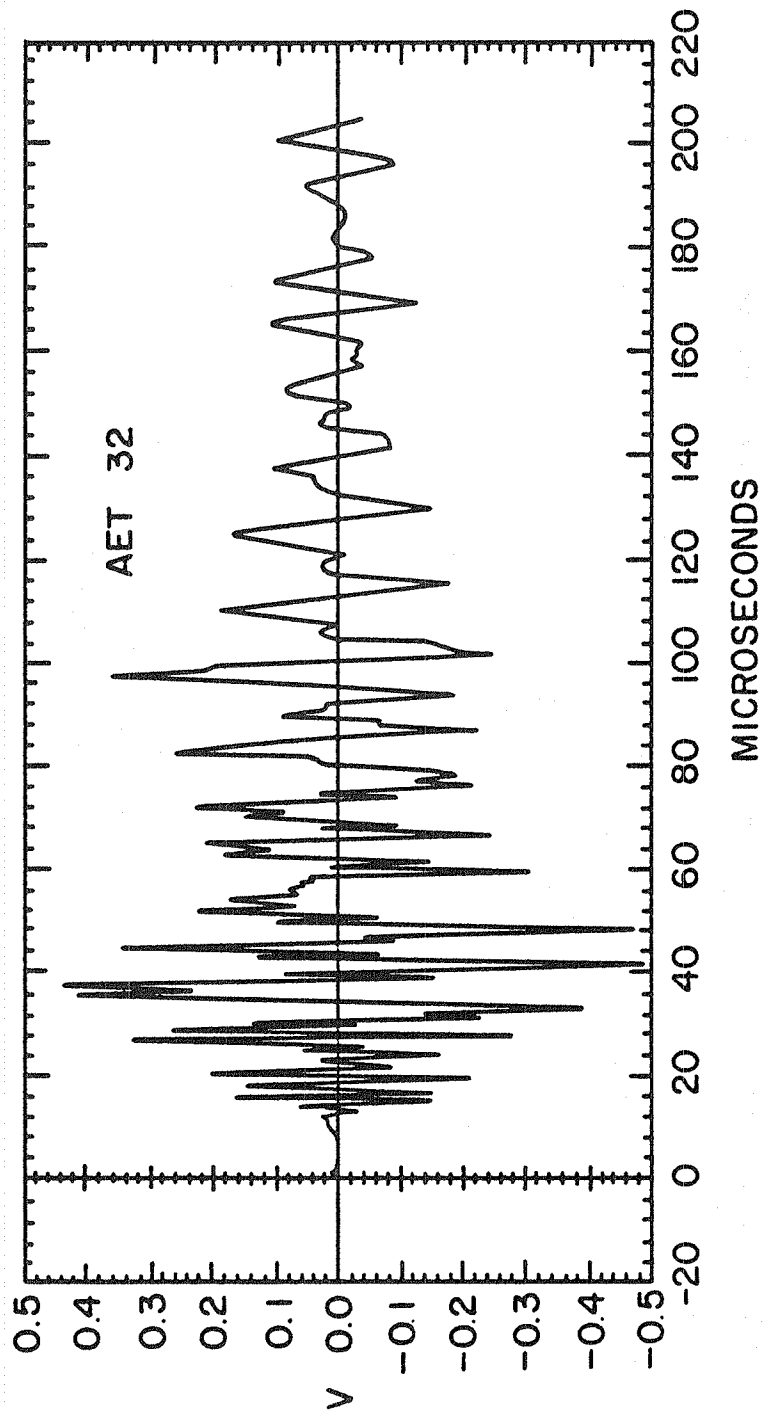


Figure 3. An individual signal used for SWF measurement in glass epoxy specimen.

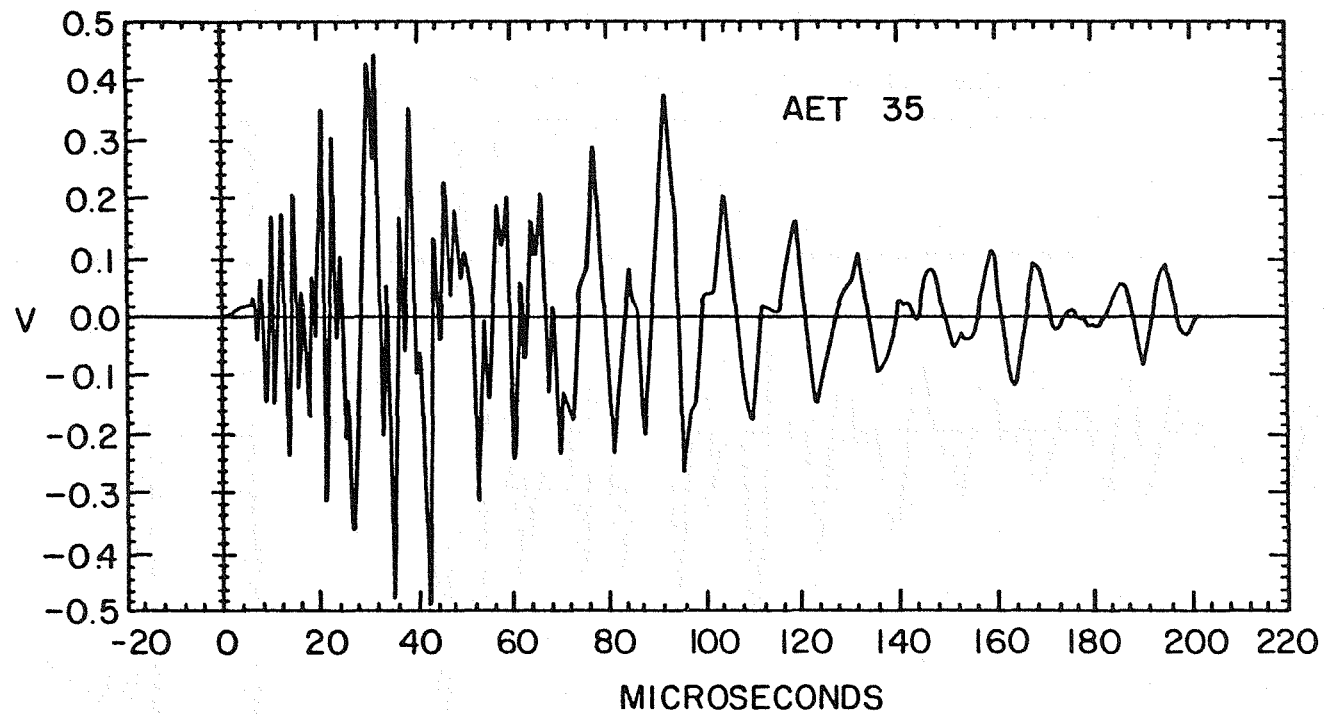


Figure 4. An individual signal recorded 20 minutes after than in Fig. 2. All other test conditions were the same.

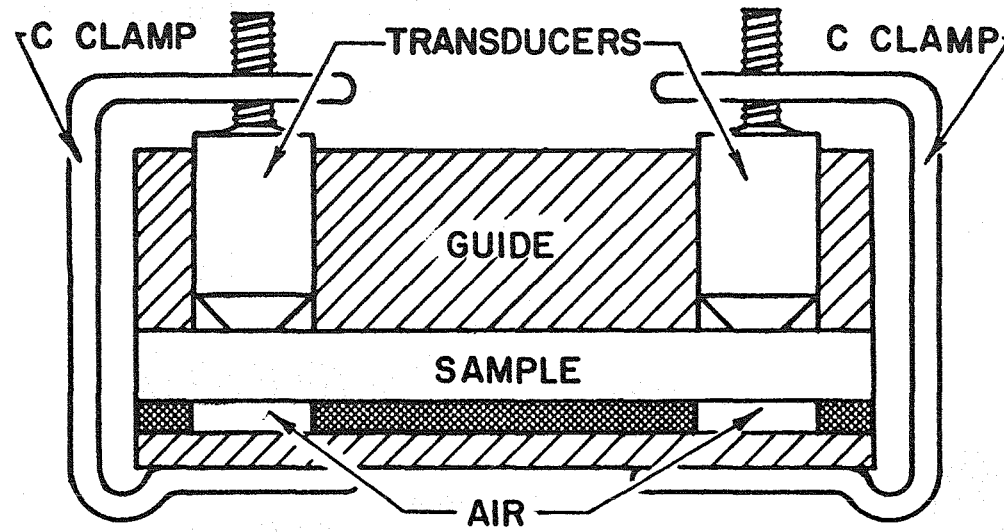


Figure 5. Schematic diagram of arrangement used to apply load to transducers and specimen.

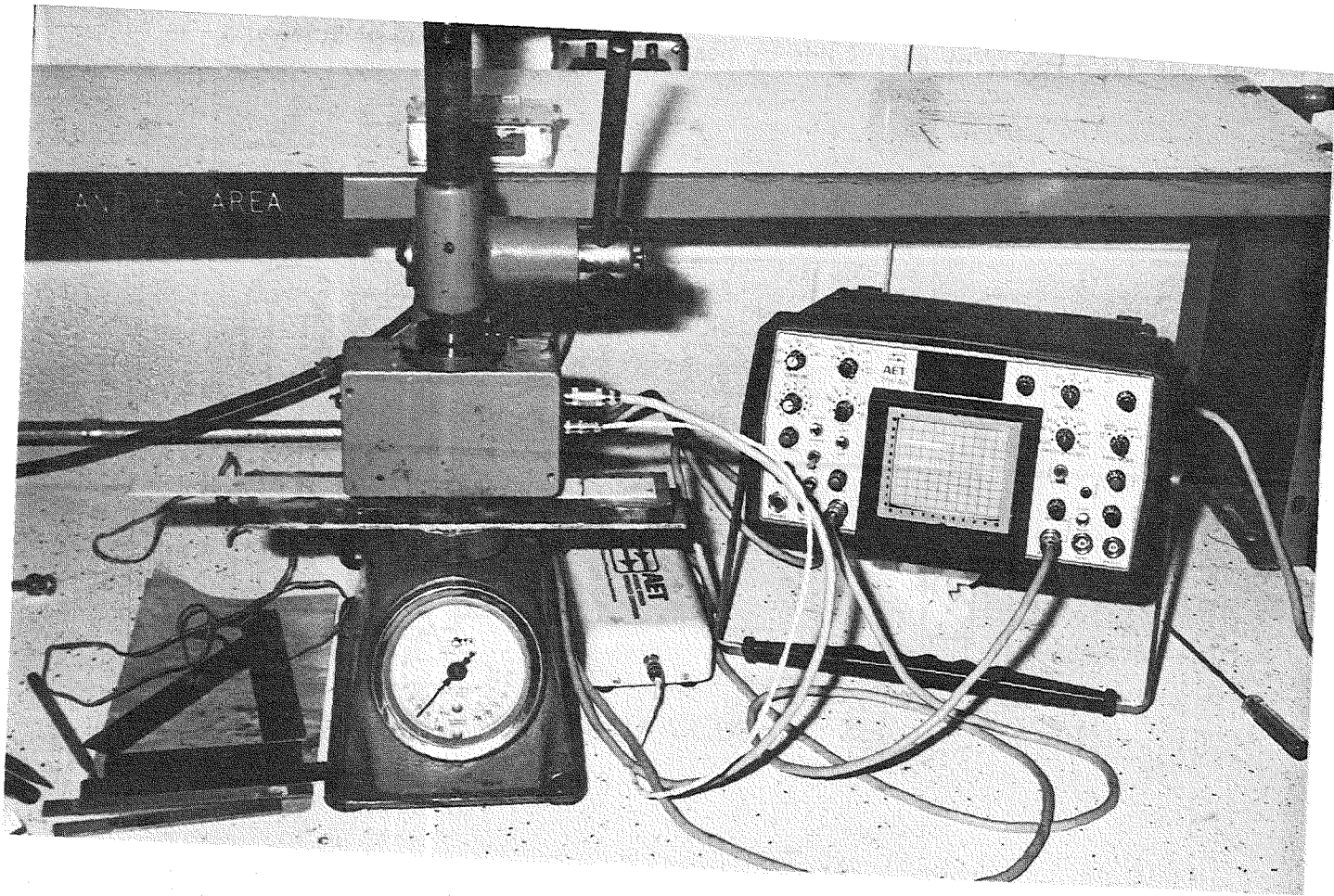


Figure 6. Photograph of spring tester used to apply load to transducers.

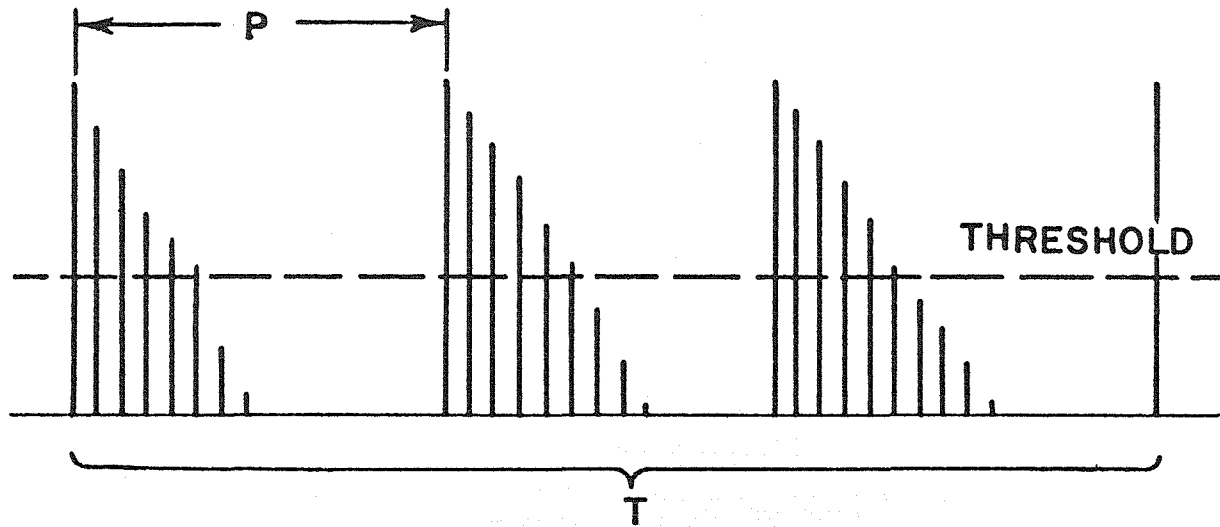


Figure 7. Schematic diagram showing parameters involved with measuring SWF.

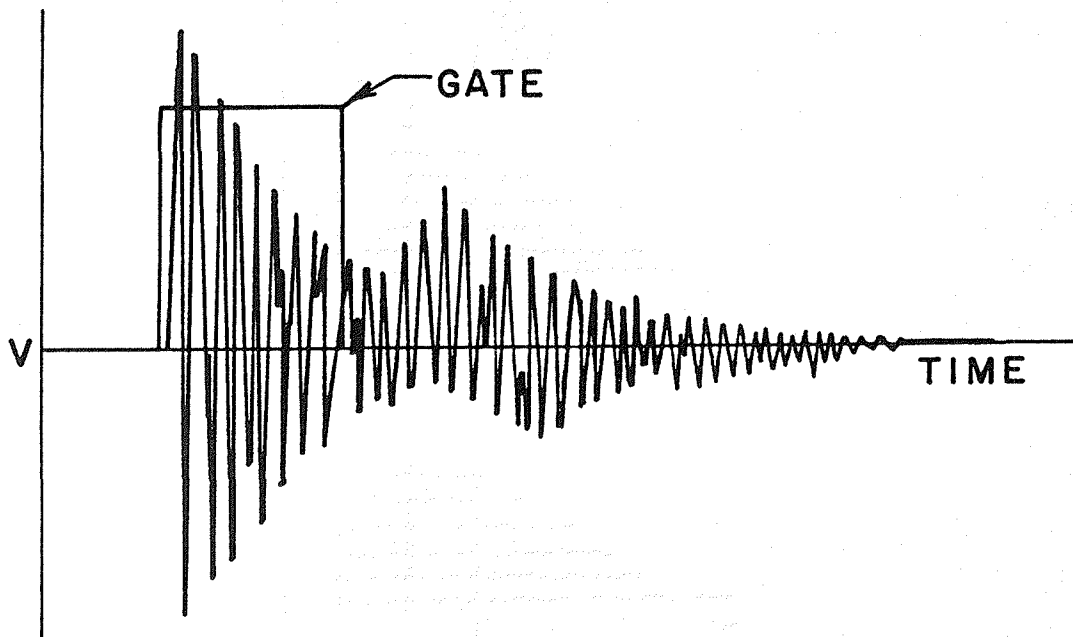


Figure 8. Schematic representation of signal-threshold-gate width interrelationship.

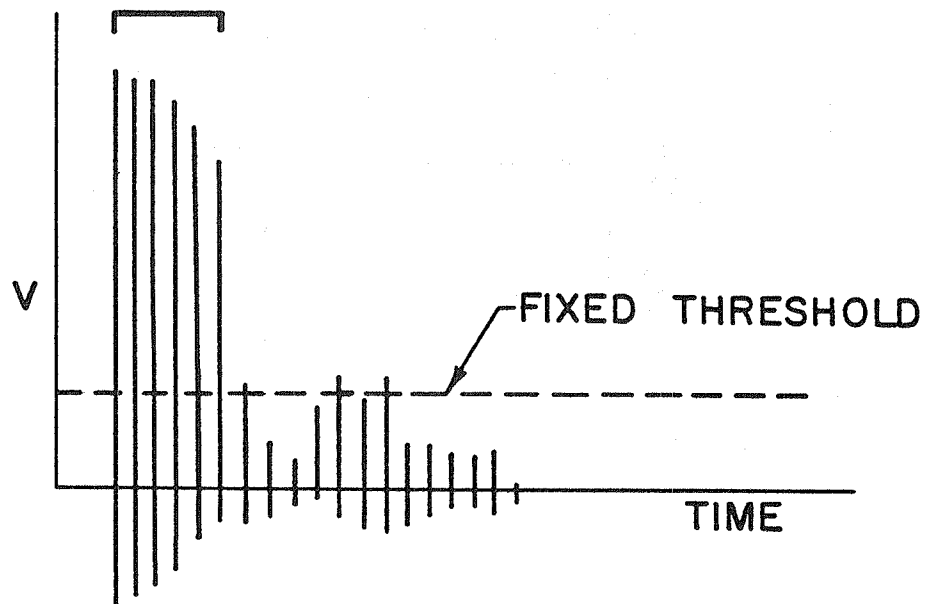
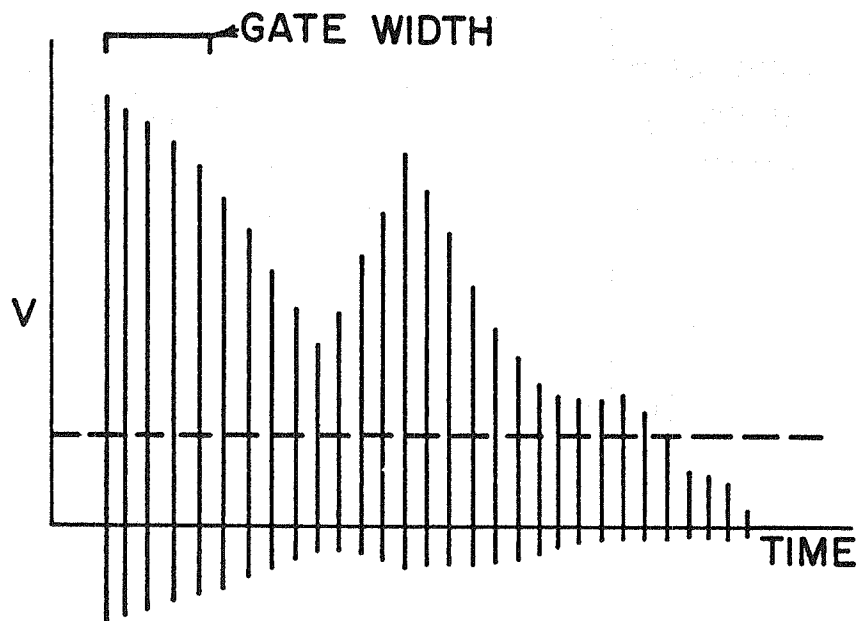


Figure 9. Two different signals yielding same SWF for sufficiently narrow gate width.

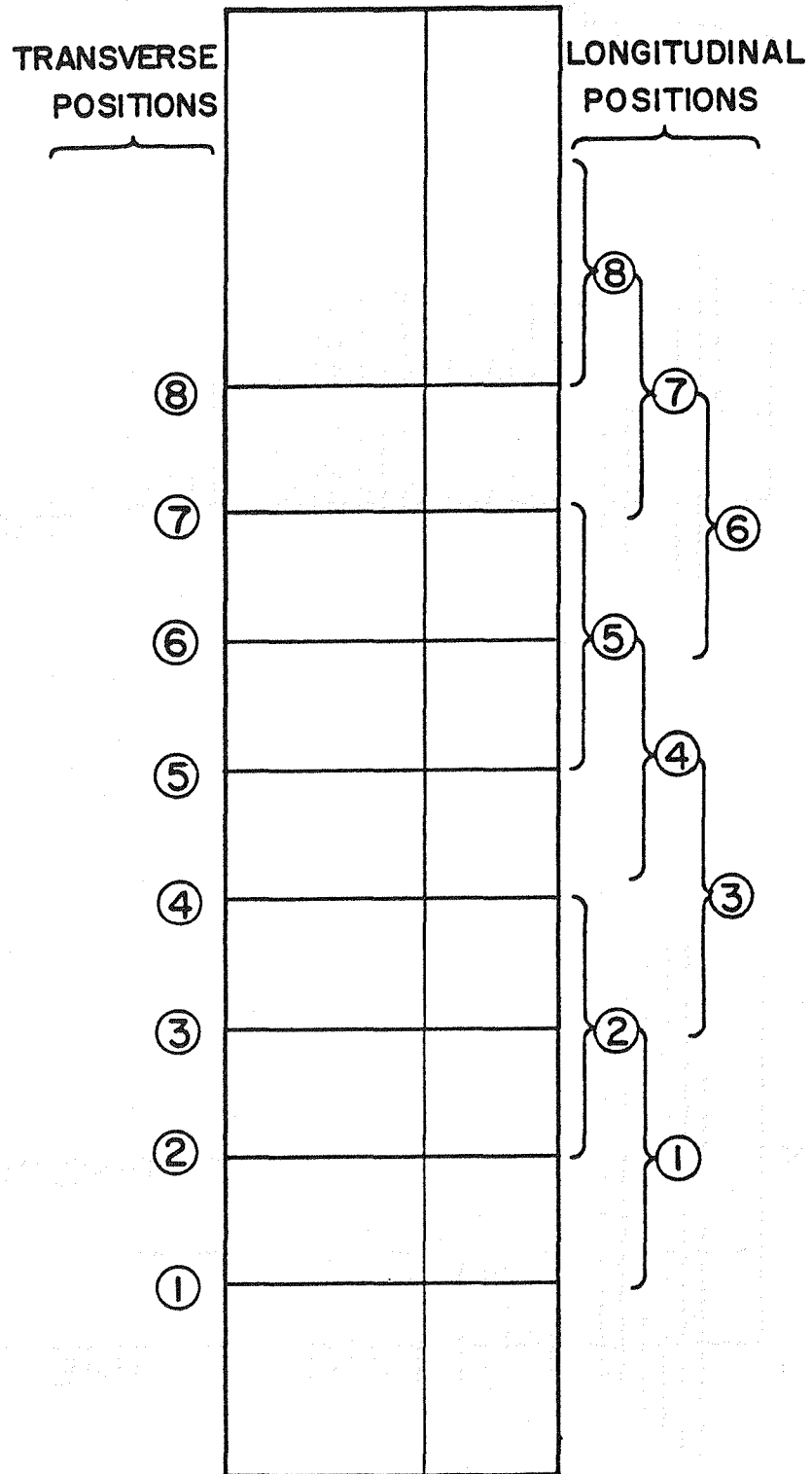


Figure 10. Longitudinal and transverse positions at which the SWF was measured.

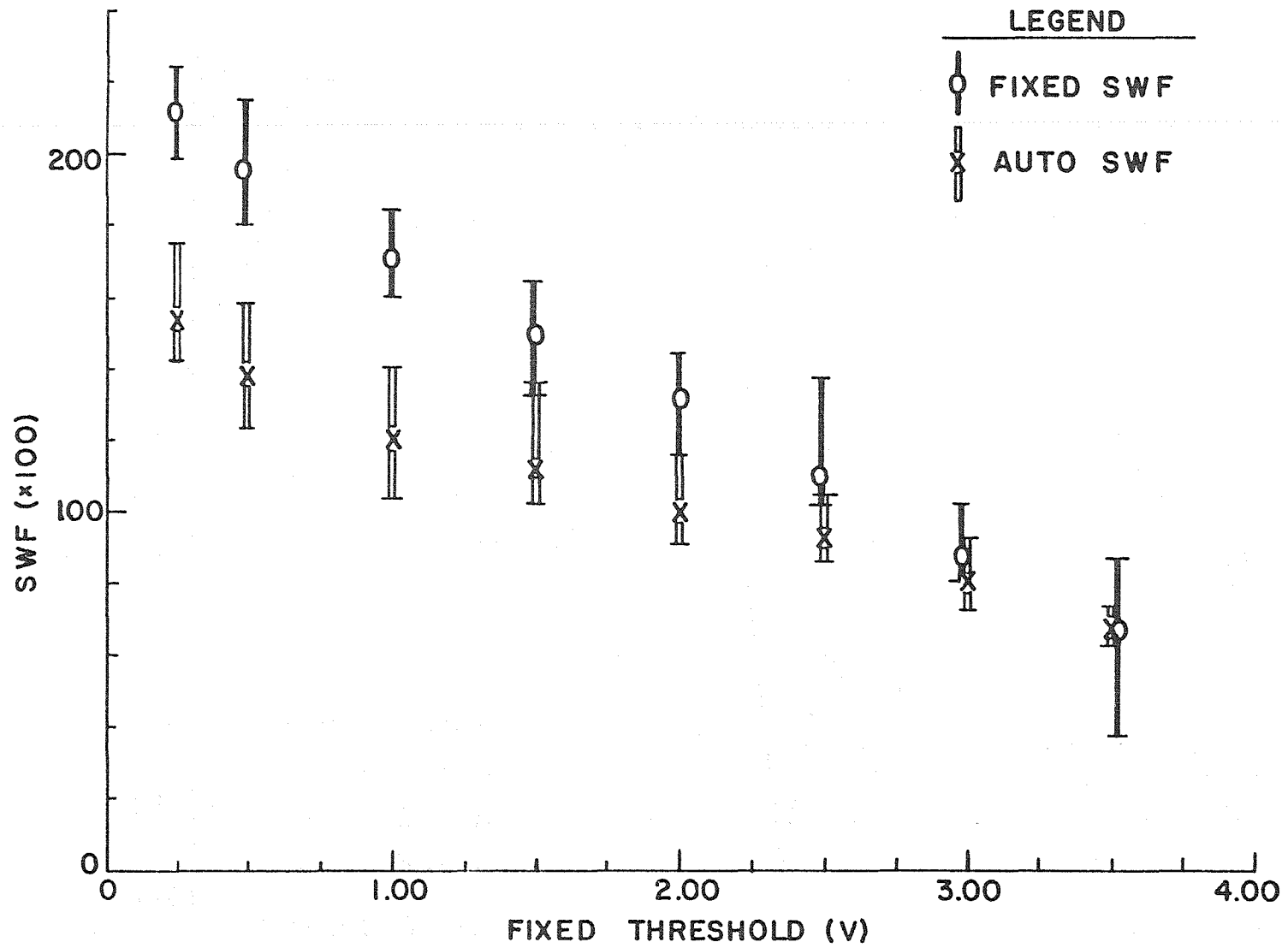


Figure 11. Typical graph showing SWF versus threshold level (transverse position 1, gate width: open).

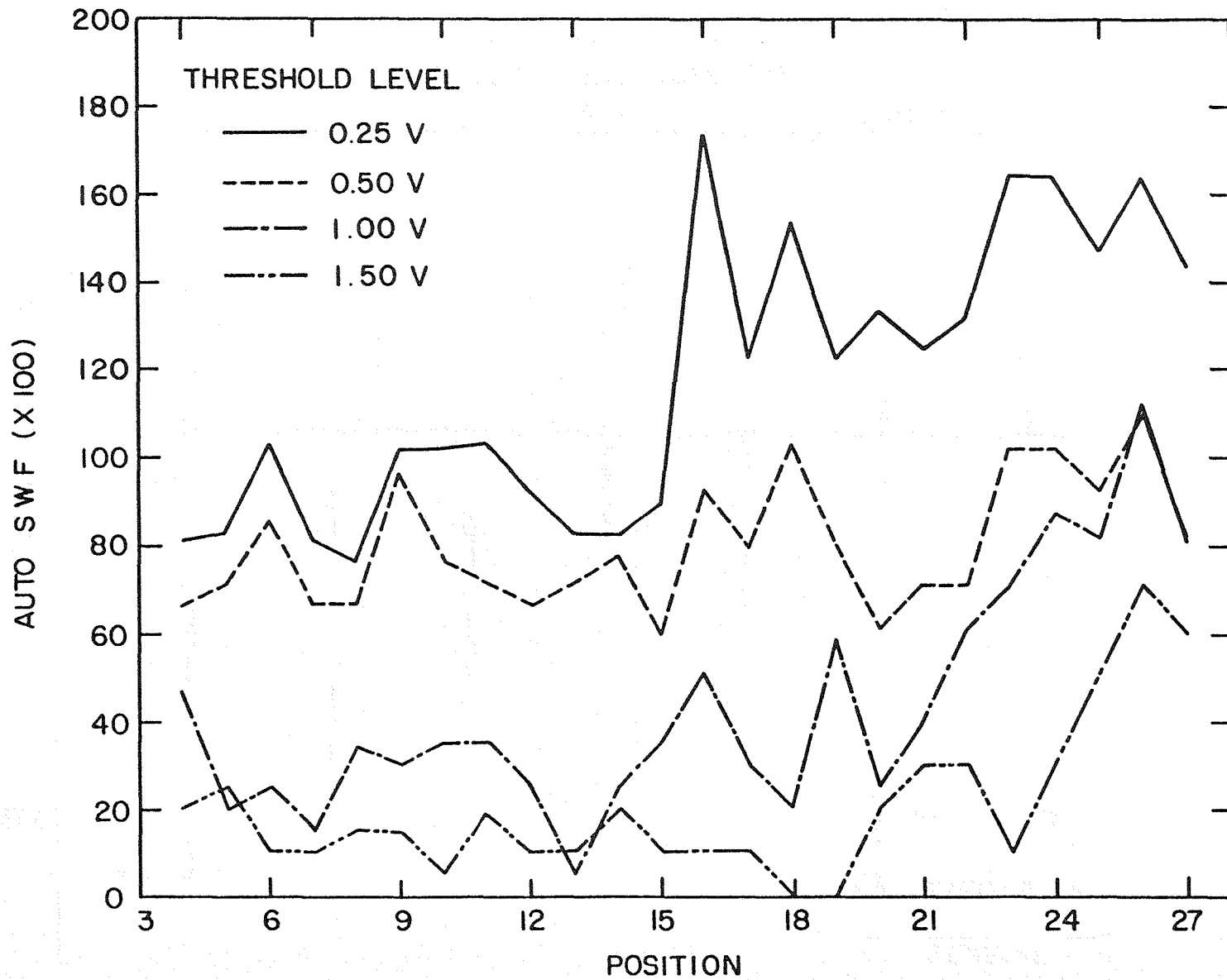


Figure 12. Typical graph showing SWF versus longitudinal position for different threshold levels.

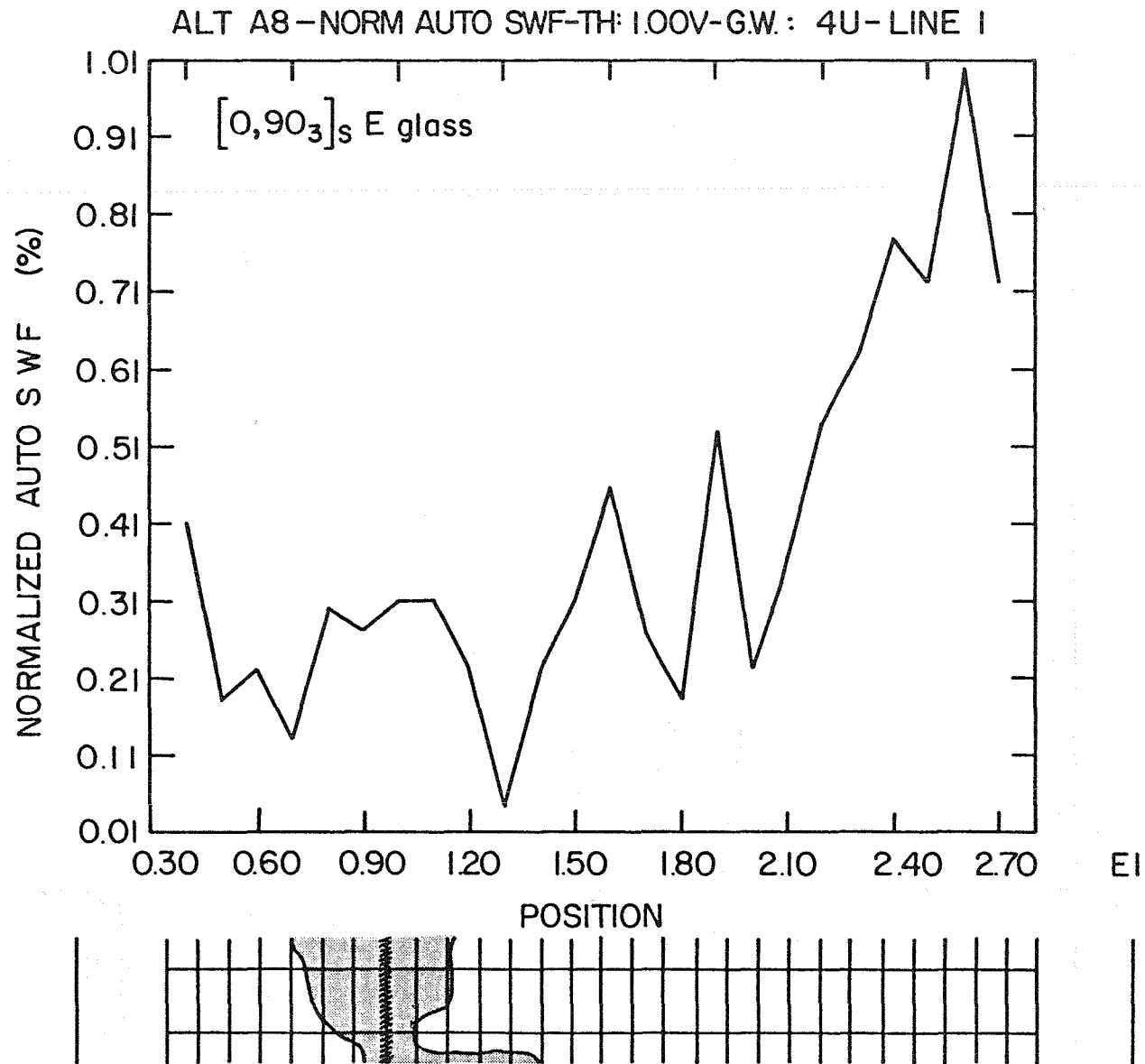


Figure 13. Correlation of longitudinal SWF with specimen failure location.

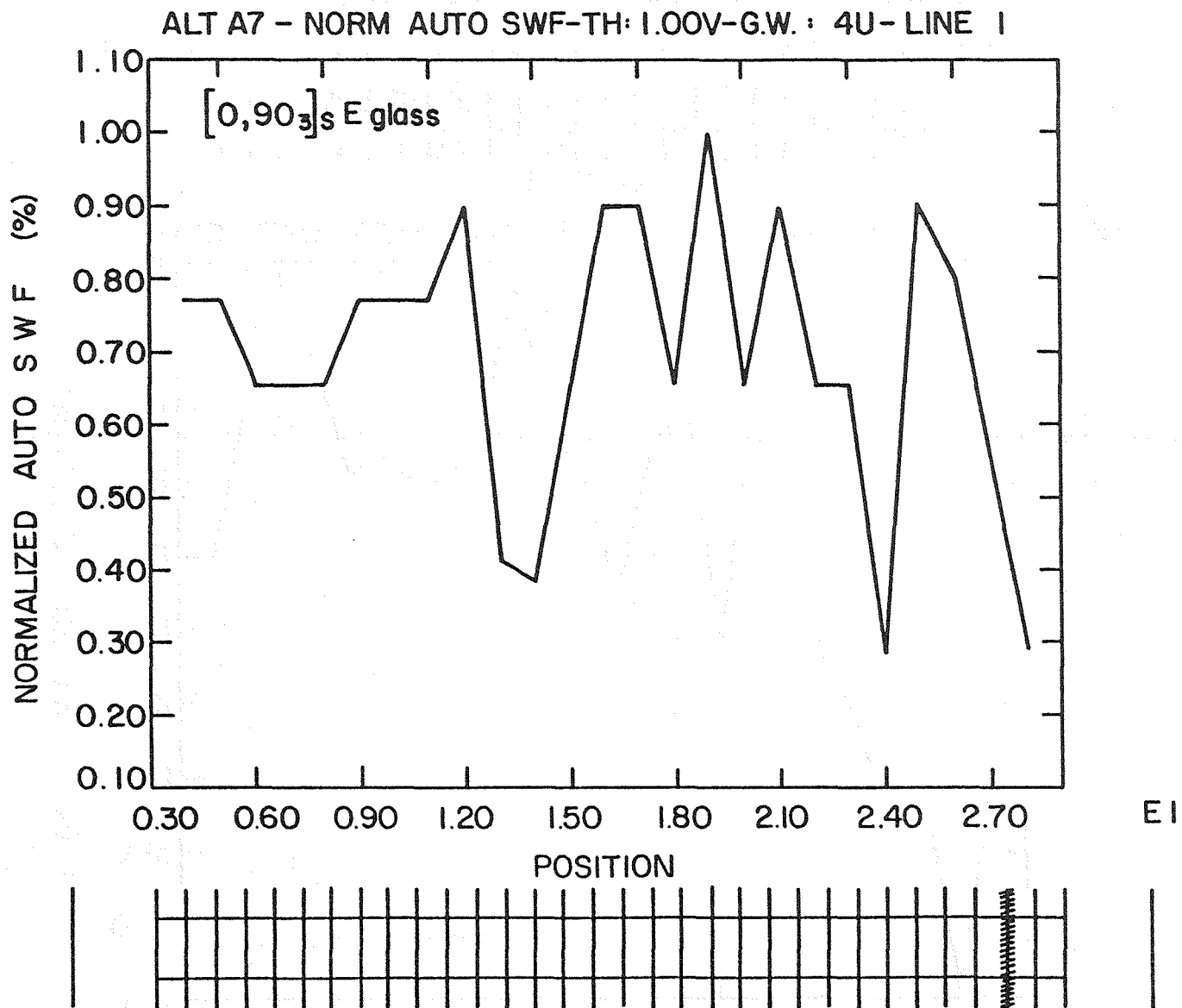


Figure 14. Correlation of longitudinal SWF with specimen failure location.

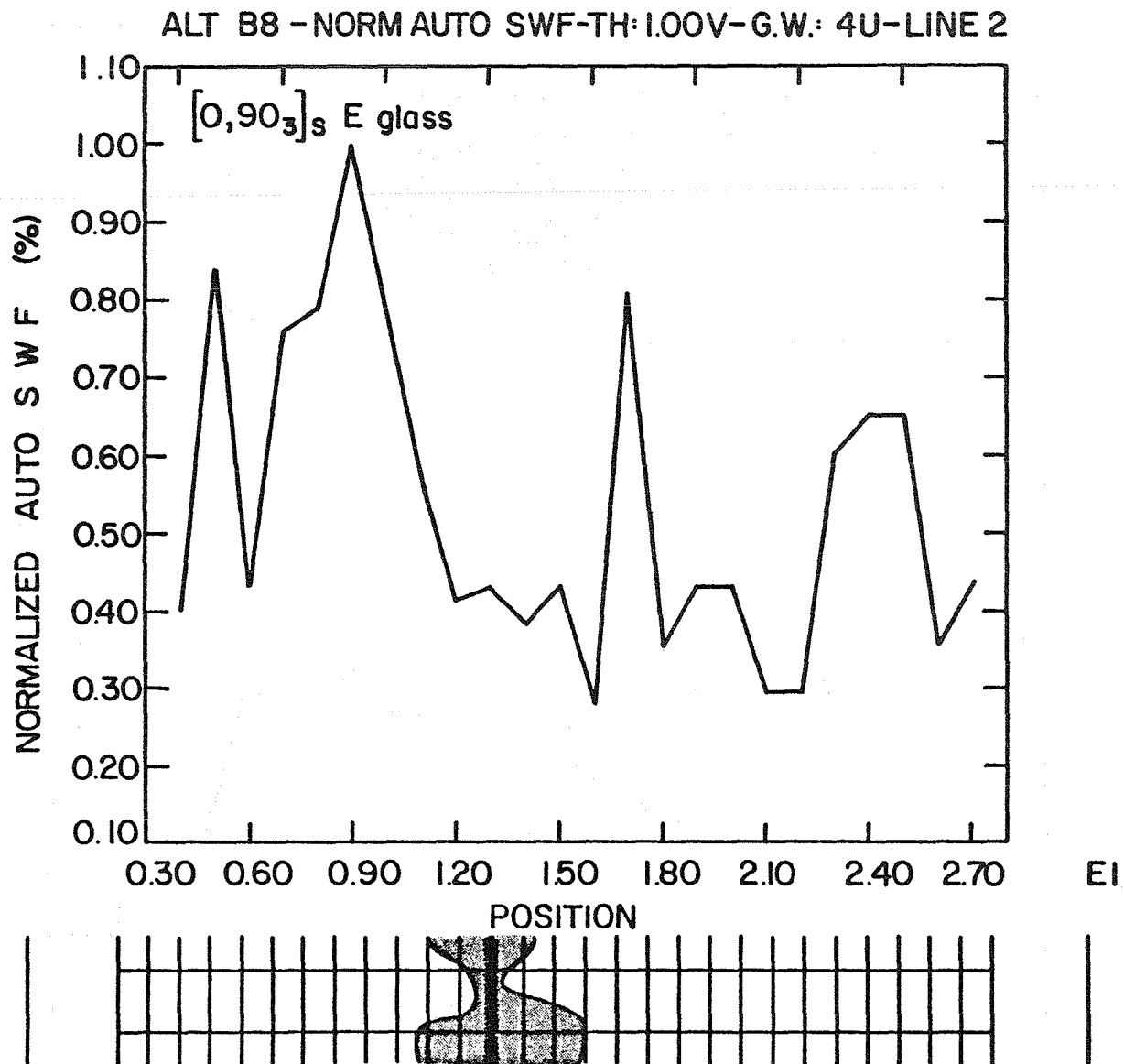


Figure 15. Correlation of longitudinal SWF with specimen failure location.

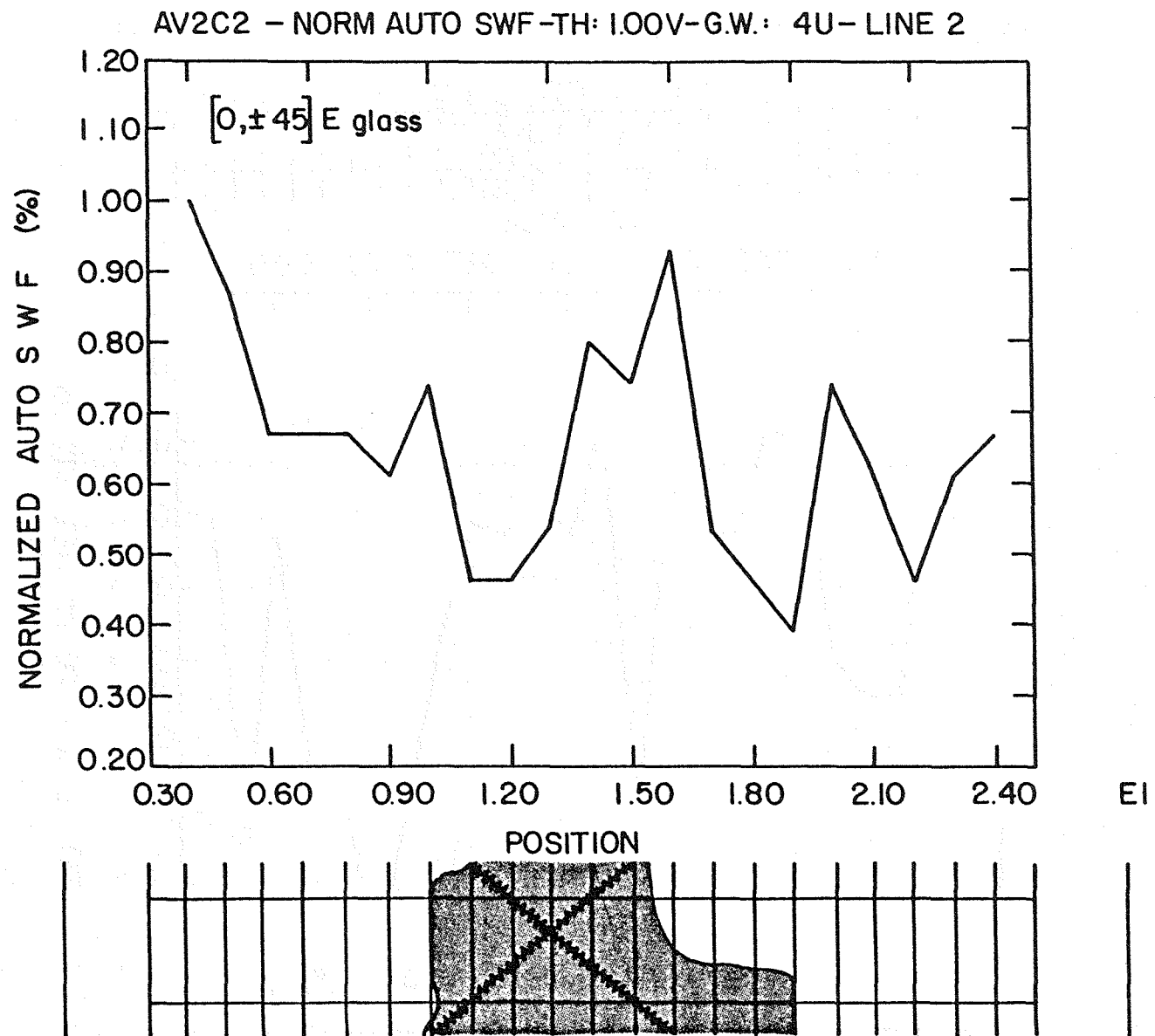


Figure 16. Correlation of longitudinal SWF with specimen failure location.

RICK 7 - NORM AUTO SWF-TH: 1.00V-G.W.: 4U-LINE 3

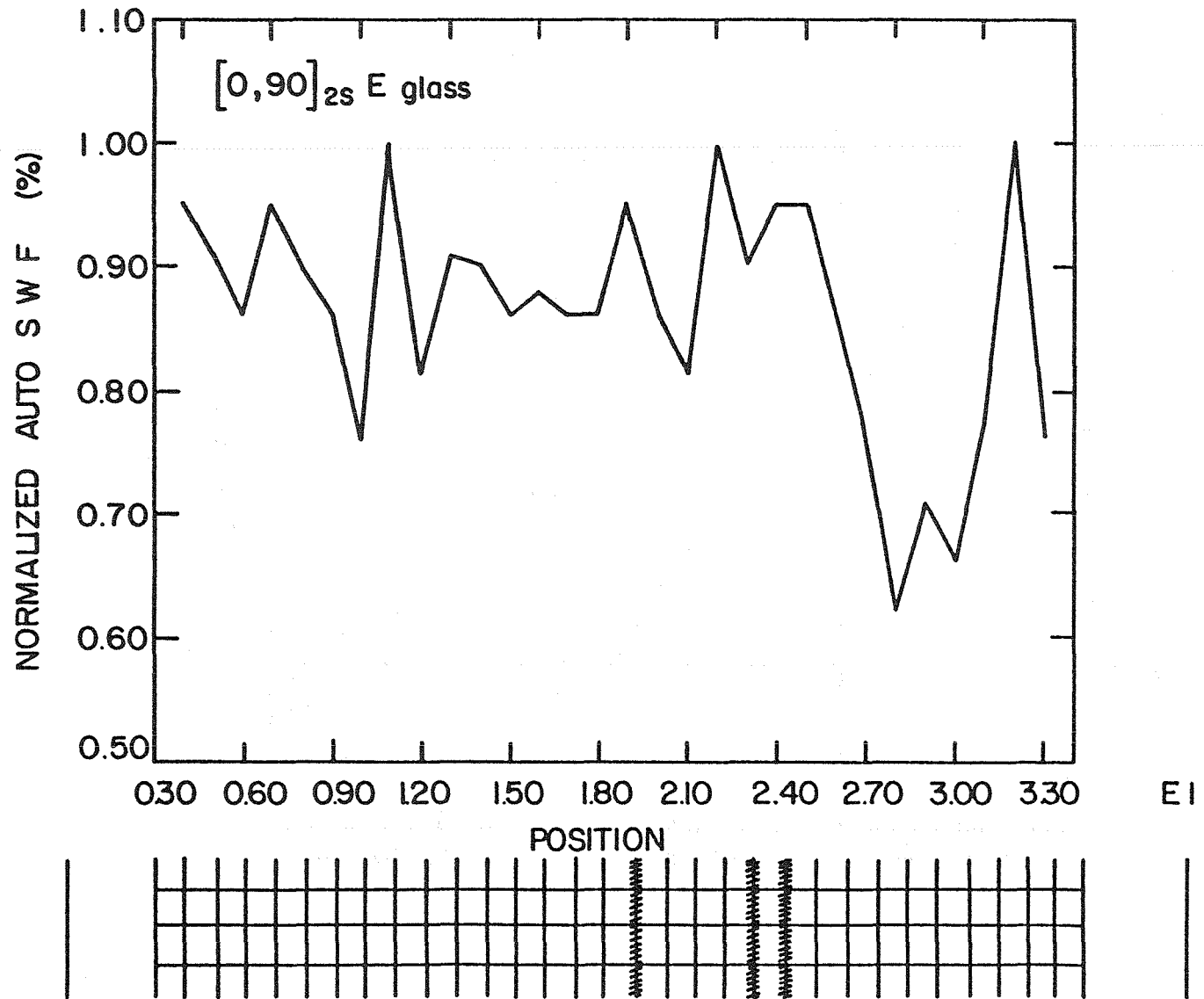


Figure 17. Correlation of longitudinal SWF with specimen failure location.

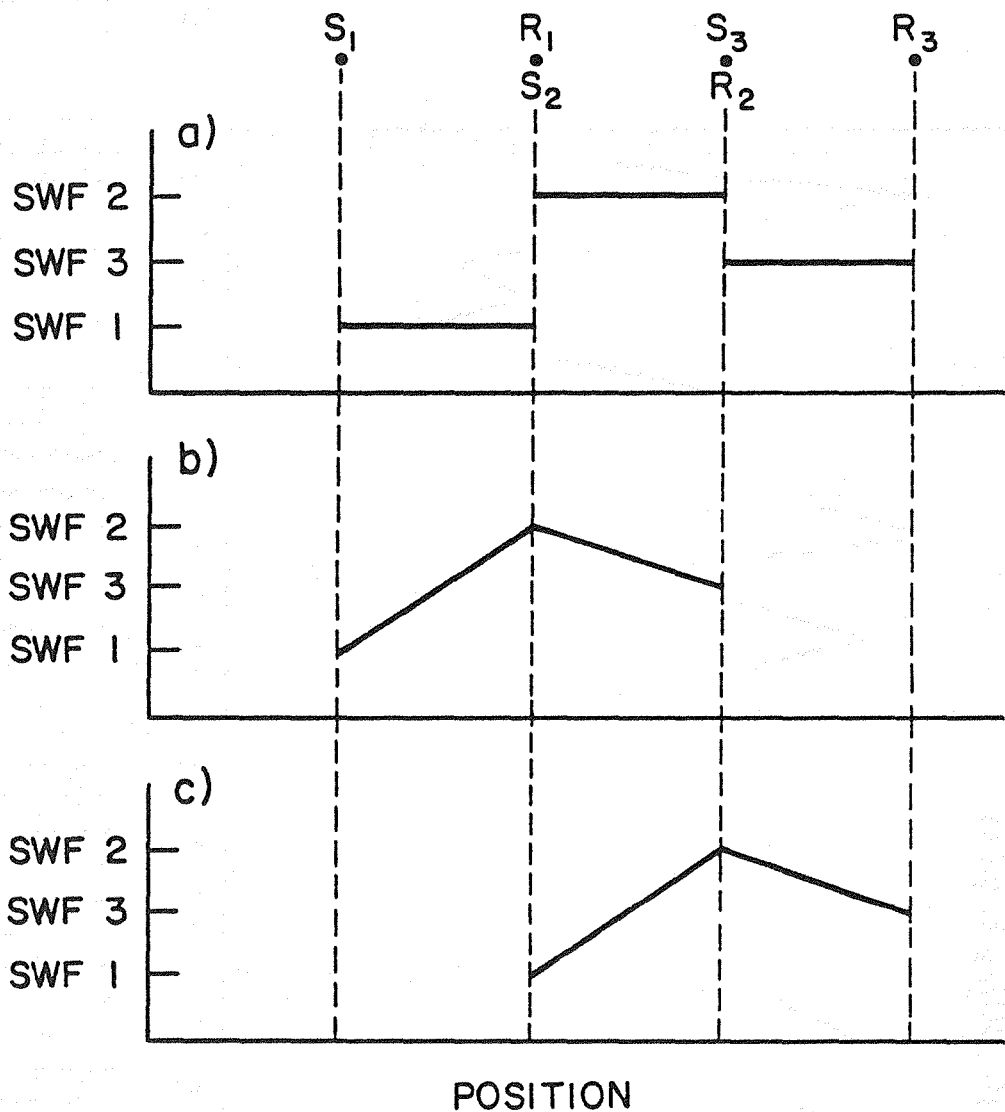


Figure 18. Schematic diagram indicating SWF measurement without any overlap of regions examined.

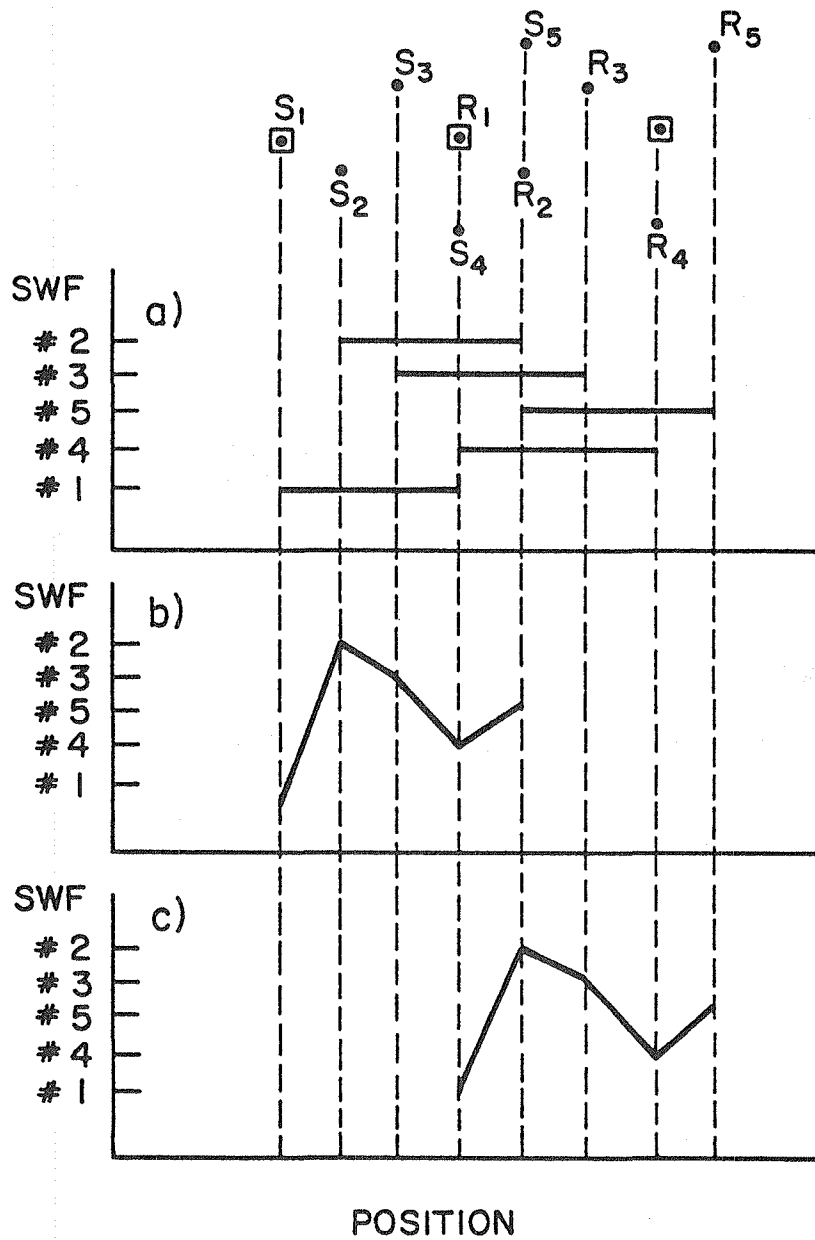


Figure 19. Schematic diagram indicating SWF measurement with overlapping examined regions.

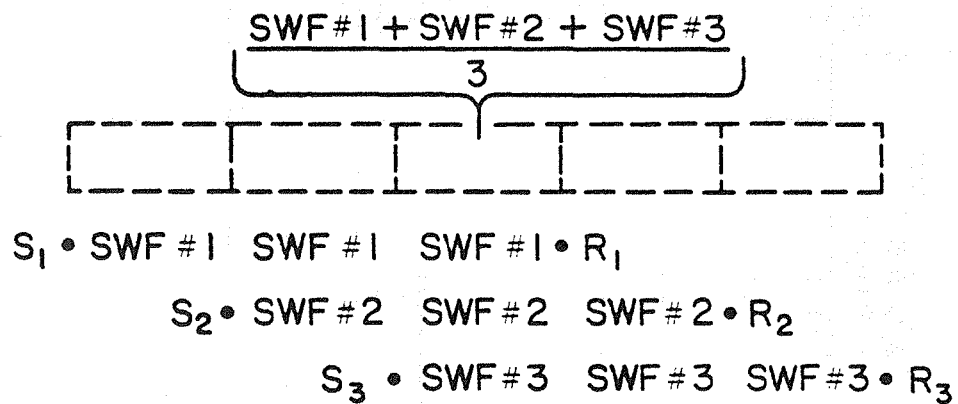


Figure 20. Weighting scheme to determine SWF value of local region in specimen. ( $S_i$ --location of sending transducer,  $R_i$ --location of receiving transducer.)

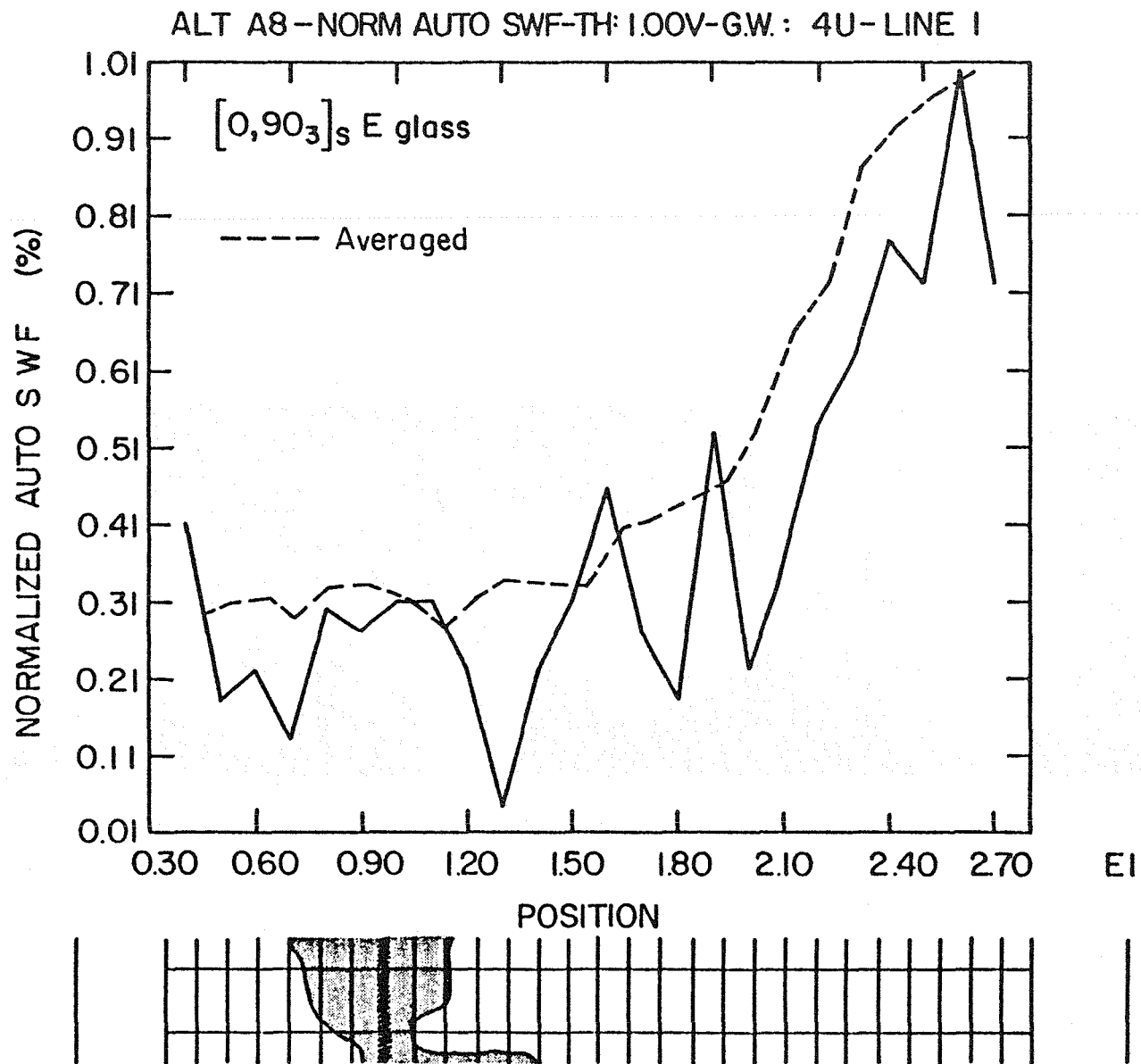


Figure 21. Comparison of SWF data from Fig. 13 with and without averaging.



Figure 22. Moiré interferometric pattern obtained when 2000  $\mu$  strain was applied to E-glass epoxy  $[0,90_3]_S$  laminate.

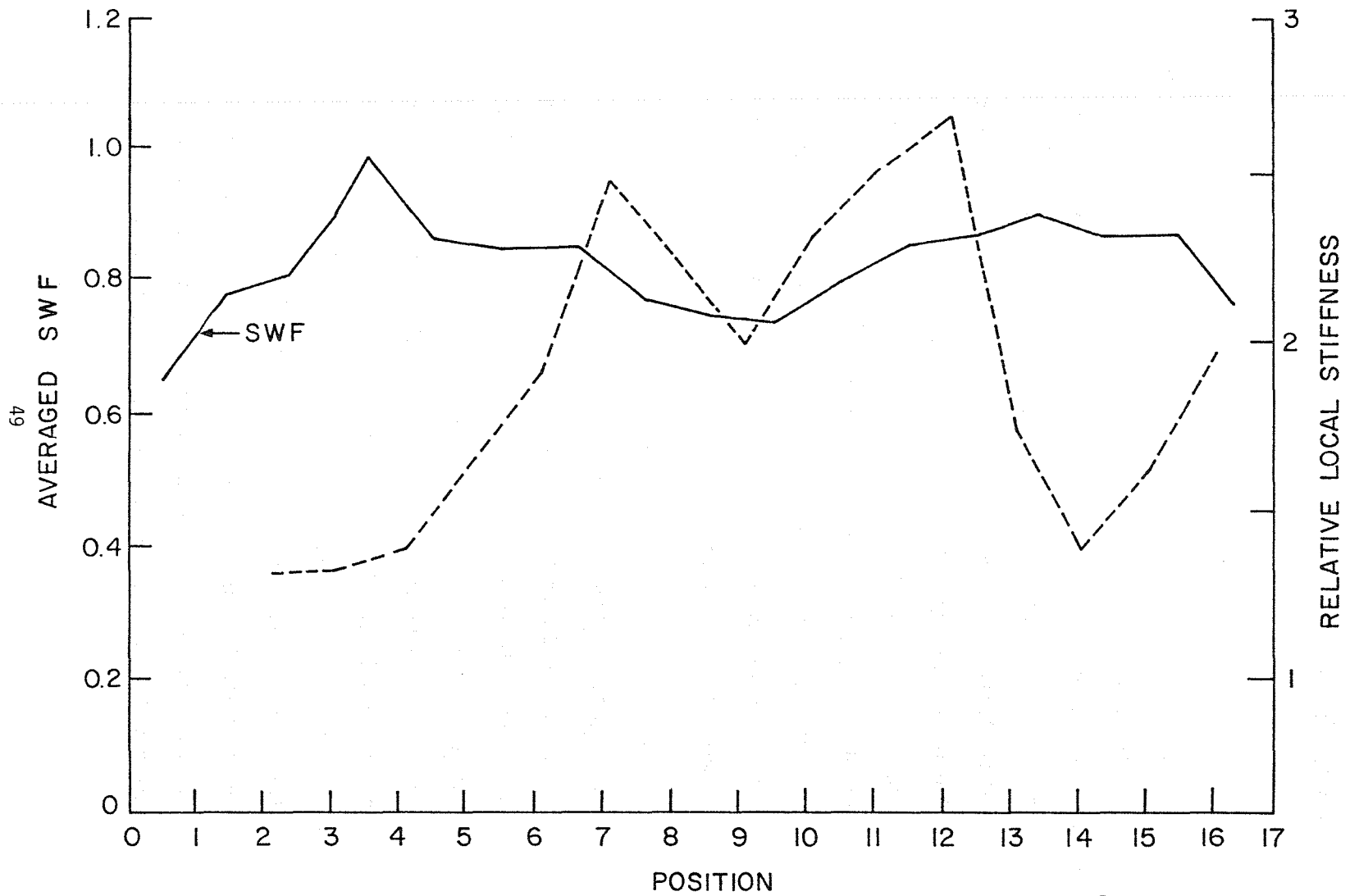


Figure 23. SWF and local stiffness variation along the length of an E-glass epoxy,  $[0,90_3]_S$  laminate.

## APPENDIX - CORRELATION OF THE STRESS WAVE FACTOR WITH MOIRÉ INTERFEROMETRY

by Anil Govada

### ABSTRACT

A  $[0,90_3]_S$  glass epoxy composite laminate, virgin specimen, was evaluated by the "Stress Wave Factor" (SWF) technique. The low values of SWF corresponding to the "weak" areas on the specimen were noted. Ultrasonic C-scans of the specimen supported the SWF results. The in-plane displacements,  $u$ , of the specimen were obtained, under load, using "Moiré Interferometry." Loading was stopped after the first ply failure of the laminate occurred. The in-plane displacements on the specimen were observed. The areas of high  $u$  displacements on the specimen corresponded quite well with the areas of low SWF. Local stiffnesses were also obtained from the moiré fringe patterns on the specimen, and correlated quite well with the SWF results.

### INTRODUCTION

#### Stress Wave Factor (SWF) -- Theory

Stress wave factor [1] is a measure of the stress wave energy transmission. The stress wave factor provides a means of rating the efficiency of dynamic strain energy transfer in a given composite material. If the material exhibits an efficient stress wave energy transfer, then it will have higher strength. That is, better stress wave transmission means better transmission of dynamic stress and load distribution. Conversely, low values of SWF would indicate places where the dynamic strain energy is likely to concentrate and promote fracture [2]. Higher attenuation gives rise to a lower SWF. In other words, the higher the SWF, the less the attenuation of stress waves.

The SWF is basically a combined ultrasonic and acoustic technique. A schematic of the SWF set up is shown in Fig. 1a. A known ultrasonic pulse is introduced at one point on the specimen and it is monitored acoustically at some other point on the same specimen. The degree of attenuation of the ultrasonic wave is converted to a numerical value called SWF after appropriate signal conditioning. The SWF itself is defined [3] as the number obtained by multiplication of the number of times the voltage level of a single signal exceeds a set threshold level by the pulse repetition rate ( $1/p$ ) and by a predetermined length of time before the counter is reset ( $T$ ). This is schematically shown in Fig. 1b.

$$SWF = C.T.\frac{1}{p}$$

where

$C$  = total number of counts of a single signal that exceeds a set threshold level

$T$  = time before the counter is reset

$\frac{1}{p}$  = pulse repetition rate

Vary et al. [1] have shown that the SWF decreased proportionally with fractional powers of ultimate strength and it may be an useful aid in predicting failure locations in thin composite laminates. They have reported data that shows final fracture of the specimen occurs at the lowest value of the SWF. This has been confirmed to a certain degree by the Materials Response Group [3] at Virginia Tech. But further work is needed to establish exactly the relationship between the various experimental parameters and the mechanical properties. The stress wave factor obtained for a given test area on a given test specimen depends on the

wave propagation direction relative to the fibers. Other factors that influence the magnitude of the value are fiber bonding, fiber-resin ratio, micro voids, interlaminar bondings, etc. The SWF obtained is a purely relative number that will differ substantially for different specimen geometries, fiber orientations, widths, thicknesses, materials, transducer pressure, coupling agent, signal gain, threshold voltage, gate width, etc. From the preliminary work that had been done at Virginia Tech, a particular set of parameters have been found to give reproducible results. The same set of experimental parameters were used in this study.

#### Moiré Interferometry (Reflection) -- Theory

Moiré interferometry depends upon diffraction of light as well as interference [4]. Moiré fringes are obtained by using diffraction gratings. A grating is a surface with regularly spaced bars or furrows. The distance between two consecutive bars is called pitch,  $g$ . Frequency  $f$  of a grating is the number of bars per unit length

$$f = \frac{1}{g}$$

A grating divides every incident wavetrain into a multiplicity of wavetrains of smaller intensities; and it causes these wavetrains to emerge in certain preferred directions. A parallel beam incident at a particular angle on the grating divides it into a series of beams that emerge at preferred angles. These beams are called diffraction orders and are numbered in sequence beginning with the zero order, which is the mirror reflection of the incident beam. The angle between the neighboring diffraction orders is small for a coarse grating and it is large

for a fine grating.

The grating equation defines the angles of diffraction, viz.,

$$\sin \theta = m\lambda + \sin \alpha$$

where  $m$  defines the diffraction order of the beam under consideration.

Coarse moiré is produced by the superposition of two coarse gratings with frequencies in the range of about 1 to 40 lines/mm. One of them is an active grating (glued to the surface of the specimen) and the other a reference grating (virtual). The virtual grating is formed by the intersection of the wavetrains from the reflective active grating and a mirror beside the active grating. Fig. 2 shows the moiré interferometry set up.

Moiré fringes are the locus of points of constant displacements, specifically the in-plane displacement component in the direction perpendicular to the lines of the reference grating [4]. Moiré fringe order,  $N$ , denotes the number of cycles of intensity fluctuation experienced at any point as the displacement changes from zero to its final value.

$$u = g N_x; \quad x = \text{longitudinal direction}$$

$$v = g N_y; \quad y = \text{transverse direction}$$

-- $u, v$  are displacements in the longitudinal and transverse directions

-- $g$  = pitch of the reference grating

-- $N_x, N_y$  are the fringe orders when lines on the reference grating are perpendicular to the longitudinal and the transverse directions, respectively.

From the displacements we can get strains

$$\epsilon_x = \frac{du}{dx}$$

$$\epsilon_y = \frac{dv}{dy}$$

$$\gamma_{yy} = \frac{du}{dy} + \frac{dv}{dx}$$

where  $\epsilon_x$  and  $\epsilon_y$  are the normal strains and  $\gamma_{yy}$  is the shear strain. Stresses can be determined using stress-strain relationships. Since the strains and the associated displacements are very small, gratings of fine pitch and high frequency are required [4].

A grating is made by exposing a high-resolution photographic plate to two intersecting beams of coherent light. Frequency of the grating is controlled by the angle of intersection according to

$$\sin \alpha = \frac{\lambda}{\alpha} f$$

where  $\alpha$  = incident angle

$\lambda$  = wavelength of light used

$f$  = frequency of grating

The two intersecting beams give rise to a diffraction pattern of light and dark bands. When the plate is developed silver grains remain in the exposed zones, while the silver is leached out in the unexposed zones. The gelatin matrix shrinks upon drying, but since it is partially restrained by the silver, shrinkage is greatest in the unexposed zones. The result is a plate with a furrowed surface which can be used as a grating. The grating is mirrorized with aluminum to improve its reflective qualities. The grating is then transferred and attached to the specimen with an adhesive.

## EXPERIMENTS AND RESULTS

### Initial Inspection

An ultrasonic C-scan of the specimen is shown in Fig. 3. There are clearly indications of flaws near the center and the top of the specimen. However, X-ray radiography and edge replications did not indicate any flaws in the material.

### Measurement of the SWF

The SWF measurements were made using a commercial instrument. Three sets of measurements were made along the length of the specimen. Fig. 4 schematically shows the orientation and various positions of the transducer assembly on the specimen. The specimen was 15cm long with an effective gage length of about 10cm. The width of the specimen was 2.5cm.

The experimental parameters used were:

Threshold	:	1.00 volts
Trig rate	:	0.5 k
Scale	:	100
Rate	:	1.0 sec
Gain	:	45 dB
Trig. mode	:	pulse
Sweep rate	:	62.5 u sec/div.
Energy	:	2.0 units
Gate	:	4 m sec
Mode	:	auto
Couplant	:	Panametrics

Distance between  
the transducers : 1.5" (fixed)

Pressure on each  
transducer : 6.82 kg

The SWF values for the various positions on the specimen are plotted in Fig. 5 (average value of all three lines). Note that the center and the ends of the specimen have low values of SWF. Fig. 6 is a 3-D plot of the SWF versus the location on the specimen.

#### Measurement of Displacements by Moiré Interferometry

Moiré fringes are obtained by superimposing a carrier pattern with a live load pattern. The carrier pattern has two functions:

1. to get easily interpretable fringes, i.e. wide apart and resolvable to the naked eye
2. to introduce apparent strain so that we can compare it with the load pattern to get relative displacement contours.

A grating of 1200 lines/mm was glued to the specimen so that the furrows on the grating were along the longitudinal axis of the specimen. The frequency of the virtual grating was 2400 lines/mm. The effective field was about 9.5cm x 2.5cm. The field size is limited by the size of the lenses. Since the gage length of the specimen under study was 10cm x 2.5cm, the field obtained here was quite adequate. The specimen was then fixed in the loading frame of the moiré interferometry setup. A carrier pattern of 10 lines/mm was initially made. The carrier pattern was taped onto a clear glass plate in the camera assembly. A superimposed view of the carrier pattern and the live pattern was obtained. At no load a perfect null field (zero fringes) is desirable but often it is difficult to achieve. In this study a perfect null field was achieved

at no load. The specimen was then loaded to various levels of strain. The strain was monitored using a strain gage cemented to the back of the specimen. A temperature compensation gage was also used to take into account the changes in strain due to thermal variations. Photographs of the superimposed carrier and the live patterns were taken at these following strains:

- 500  $\mu\epsilon$  . . . . . Fig. 7a
- EM 1800  $\mu\epsilon$  . . . . . Fig. 7b
- 2000  $\mu\epsilon$  . . . . . Fig. 8a
- EM 2300  $\mu\epsilon$  . . . . . Fig. 8b

EM denotes that extensional mismatch had been introduced at these strains. This is necessary when the fringes are so close together that the human eye cannot resolve them. The extensional mismatch introduced, removes the average displacements from the fringe pattern, so that fringes remain only in the high displacement areas. Extensional mismatch can be introduced by changing the angle at which the beam is incident upon the specimen. When strains are computed from displacements, care should be taken to account for the average displacements that have been removed.

Measurement of Local Stiffnesses

The moiré pattern at 2000  $\mu\epsilon$  was used to measure the local strains at each node point on the specimen. There are seventeen node points for each line along the length of the specimen. There are three lines; see Fig. 4. Two-thousand  $\mu\epsilon$  was chosen, as this level of strain did not fail the 90° plies in the laminate. As the axial load on the specimen

was constant, the reciprocal of strain would essentially be the stiffness. The stiffness values were measured at all fifty-one (17x3) points on the specimen. Fig. 9 shows a plot of local stiffnesses versus the position on the specimen.

### Discussion

Observing Fig. 7a and 7b one may see that upon increasing the strain, the displacement contours gradually changed from a uniform field, Fig. 7a to a nonuniform one, Fig. 7b. At 2000  $\mu\epsilon$ , Fig. 8a, which is a little lower than the failure strain for 90° plies in the specimen shows high displacements near the center and the ends as indicated by fringes that are closely spaced. The area above and below the center had lower number of fringes corresponding to lower displacements. Note that the moiré fringes cannot be clearly seen at the bottom end of the specimen because of an irregular scrim cloth pattern which resulted from the specimen fabrication. From the moiré fringes it is clear that the weak areas obtained with the SWF technique (Fig. 5) at the center and the ends of the specimen correspond to regions where the displacement contours are closely spaced. That is, areas of high displacement correspond to low stress wave energy transmission: such a behavior might be expected of weak regions. At 2300  $\mu\epsilon$ , Fig. 8b, at which the 90° plies failed there was some rotation of the fringes, but the fringes were still closely spaced at the center and the ends of the specimen. From Fig. 9, it is clear that the positions of low SWF correspond quite well with the areas of low stiffnesses on the specimen. From these results it can be suggested that the variation of strain energy density could be related to

the energy transmission (SWF) in this specimen. The variation of strain energy density can be evaluated from the moiré patterns. Variation of strain energy density is work, and this can be related to the SWF.

The specimen after being removed from the load frame of the moiré interferometry set up was pulled in quasi-static tension until final fracture. The specimen failed in the top grip. As a result, we cannot make meaningful correlations between this fracture, the displacement contours and the SWF values measured earlier. The interpretation of a failure in the grip region is complicated even more by the complex stress state caused by the grips. However, it is interesting to note that the top grip region had low values of SWF; see Fig. 10.

Future work recommended includes the measurement of both  $u$  and  $v$  displacement fields and the development of a model based on the variation of strain energy density and the SWF.

### Conclusions

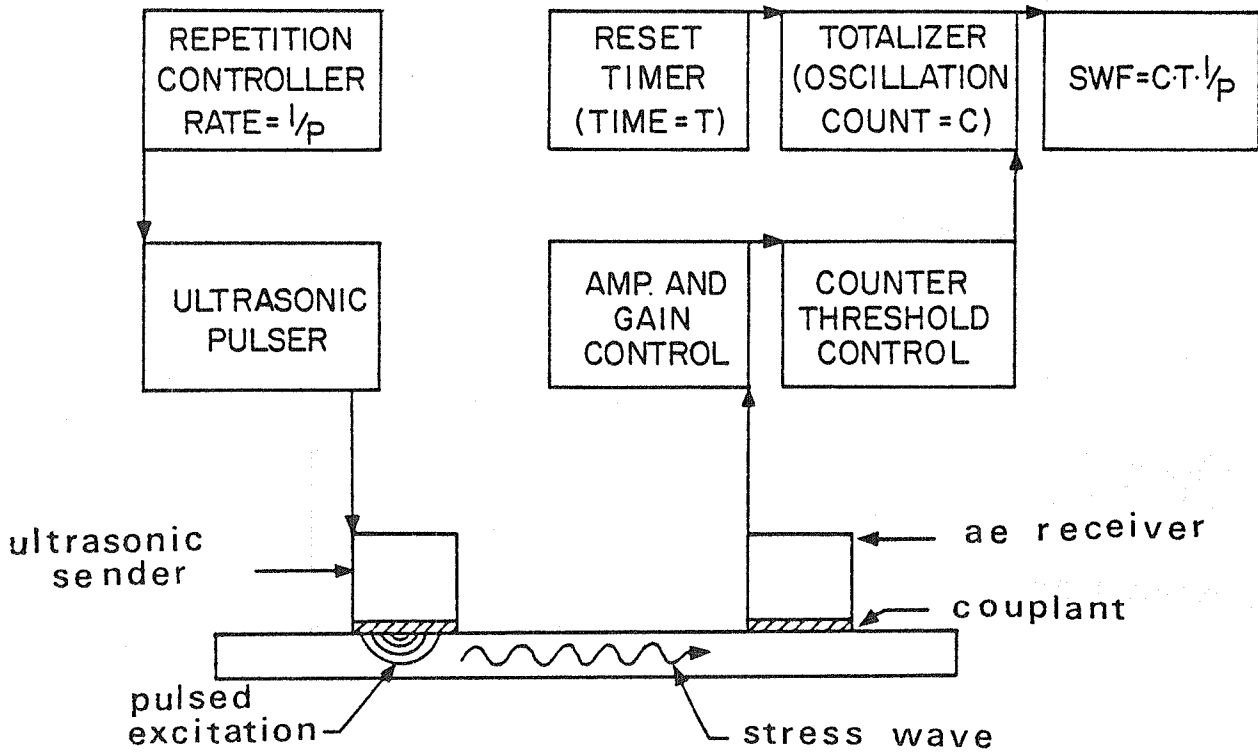
The conclusions from this study are:

1. Moiré interferometry is a useful method to check the validity of the SWF results, as there was an excellent correlation between these two techniques.
2. Local stiffness values obtained from the moiré fringe patterns correlated quite well with the SWF results.
3. A correlation between the initial C-scan and the SWF results was observed.

#### REFERENCES

1. Vary, A. and Lark, R. F., "Correlation of fiber composite tensile strength with the ultrasonic SWF," Technical paper presented at ASNT Spring conference, 1978.
2. Vary, A., "Concepts and techniques for ultrasonic evaluation of material mechanical properties," Technical paper presented at the Mechanics of NDT Conference held at VA Tech, 1980.
3. Henneke, E. and Lemascon, A., "Examination of the stress wave factor technique for NDE of composite laminates," Technical paper presented at ASNT Fall conference, 1981.
4. Post, D., "Optical interference for deformation measurements-- classical, holographic and moiré interferometry," Technical paper presented at the Mechanics of NDT Conference held at VA Tech, 1980.

a) Schematic of the SWF experimental setup.



b) Definition of SWF.

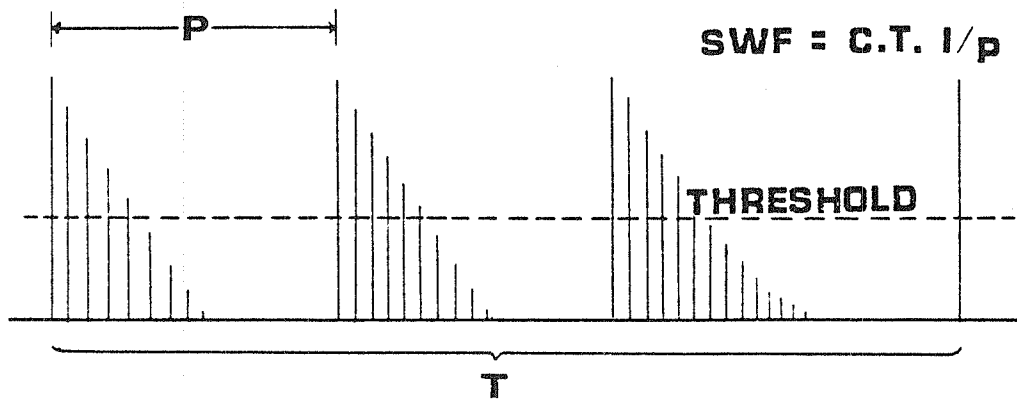


Figure 1. - Diagrams for SWF measurement.

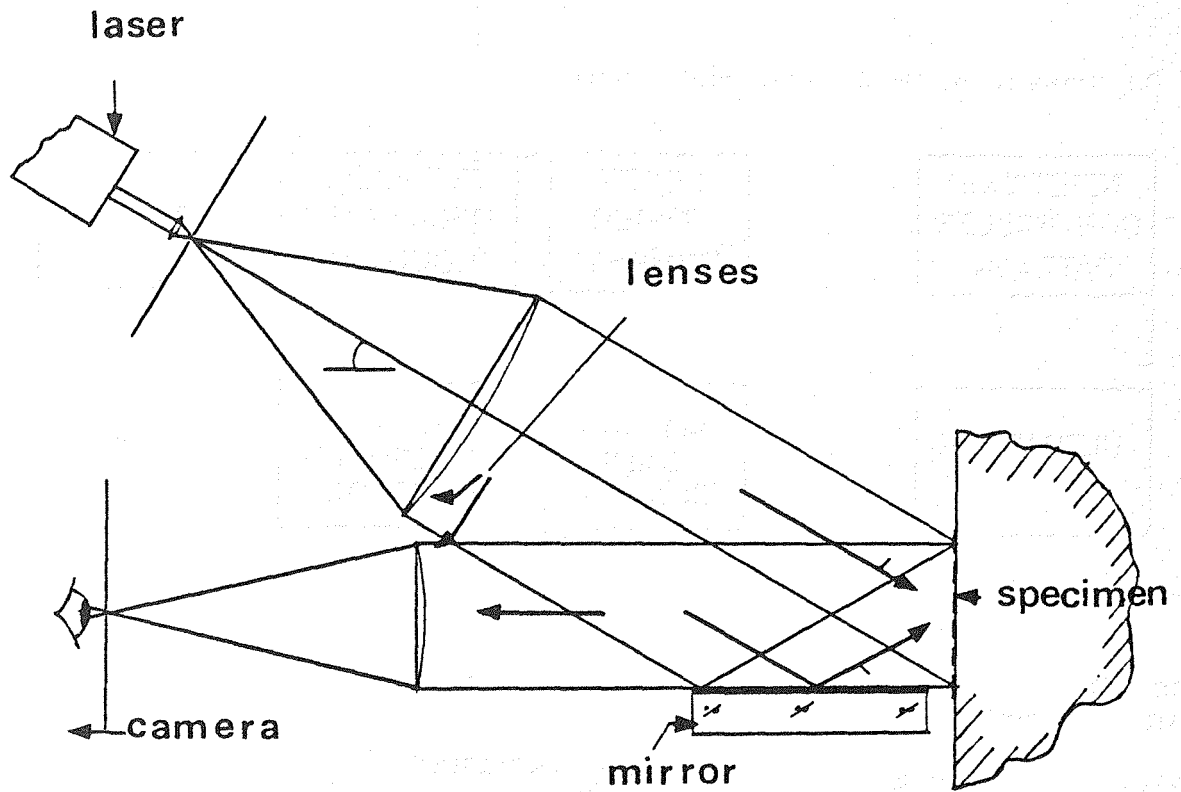


Figure 2. - Schematic of moiré interferometry setup.



Fig. 3 Ultrasonic C-scan of a virgin  $(0,90_3)_S$  E-glass epoxy specimen. Note indication of flaws at the center and the top of the specimen.

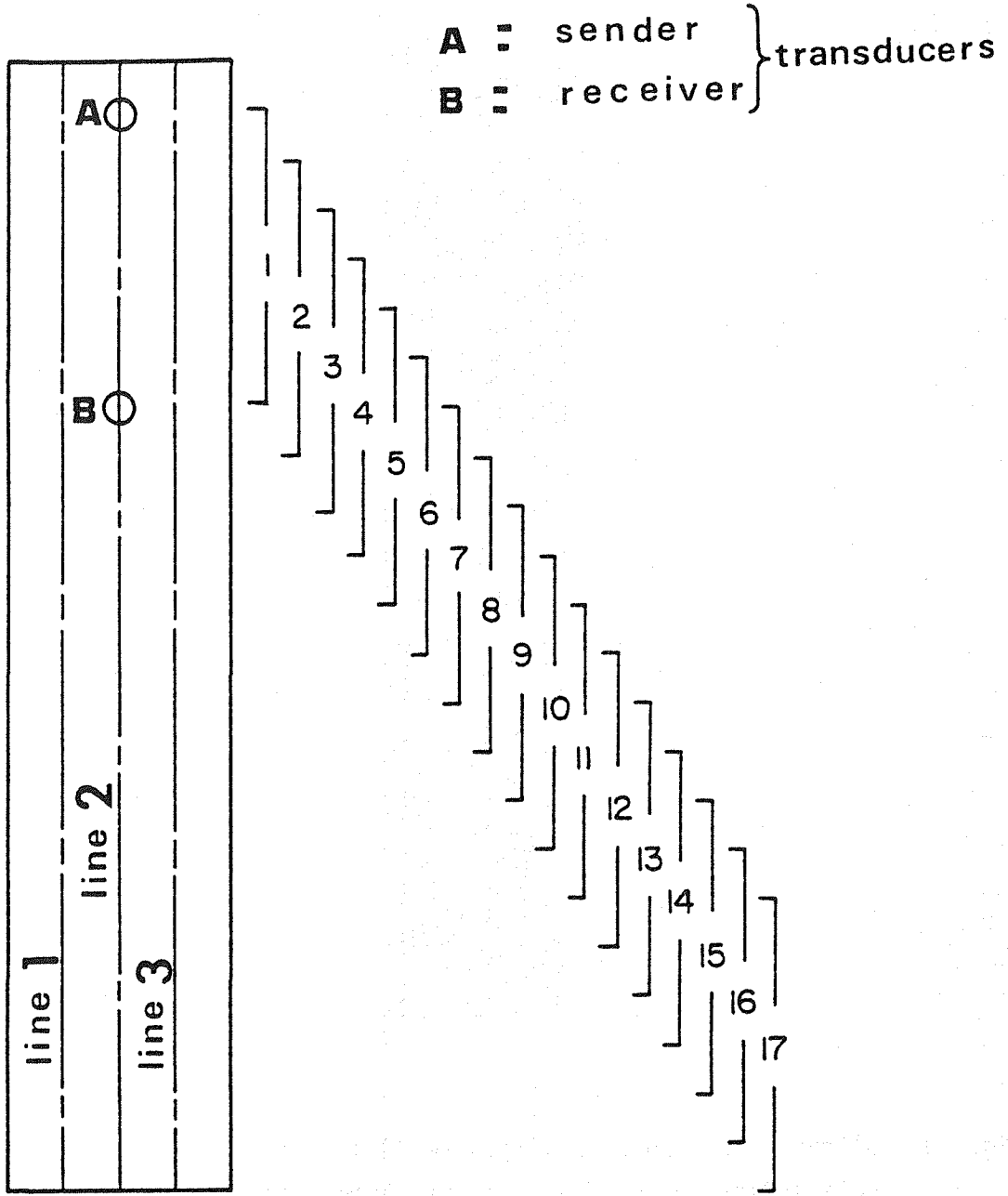


Figure 4. - Schematic showing the location of the SWF measurements made on the specimen.

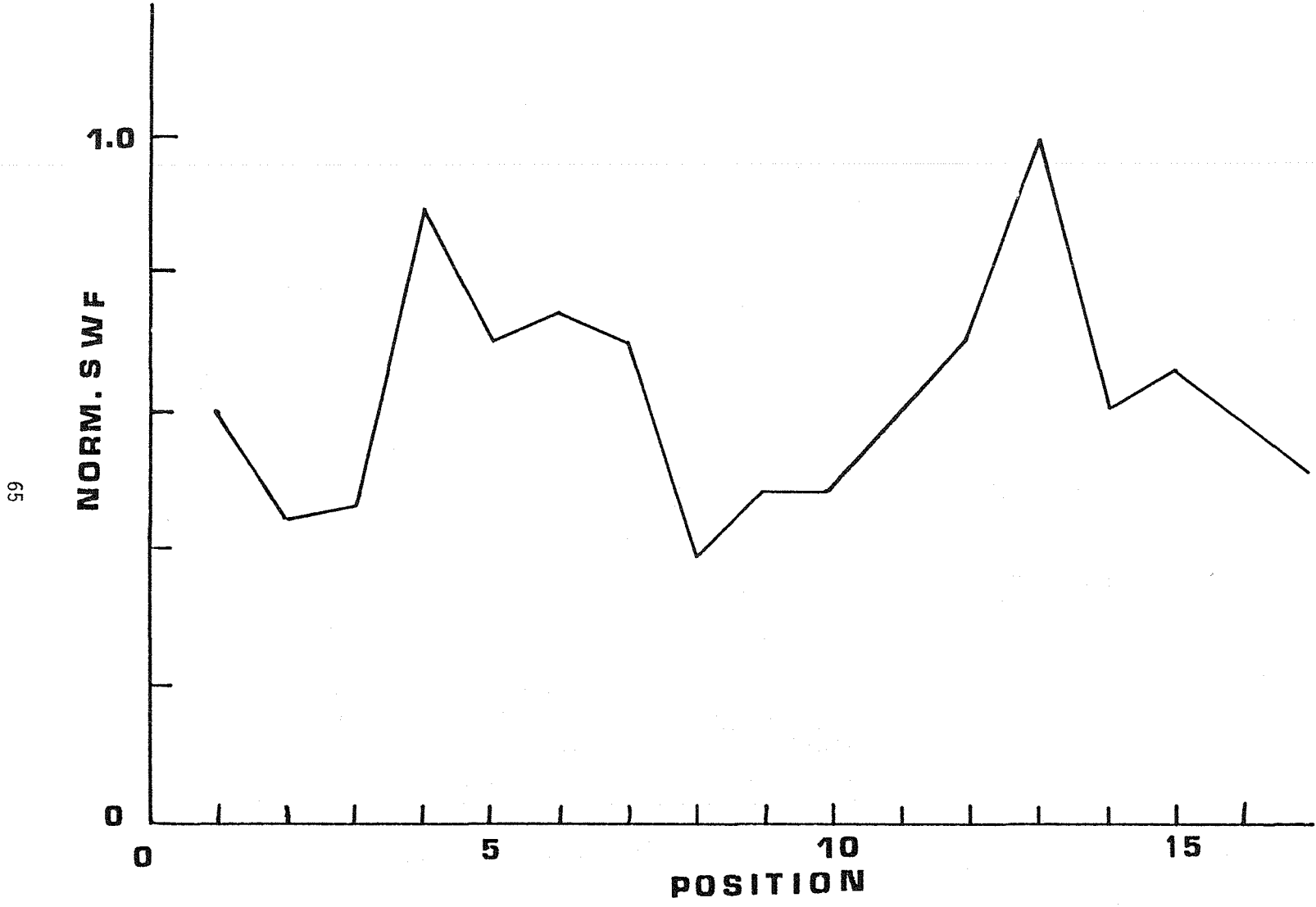


Figure 5. - Plot of average (normalized) SWF vs. position on specimen. Low values of SWF indicate weak regions and vice versa.

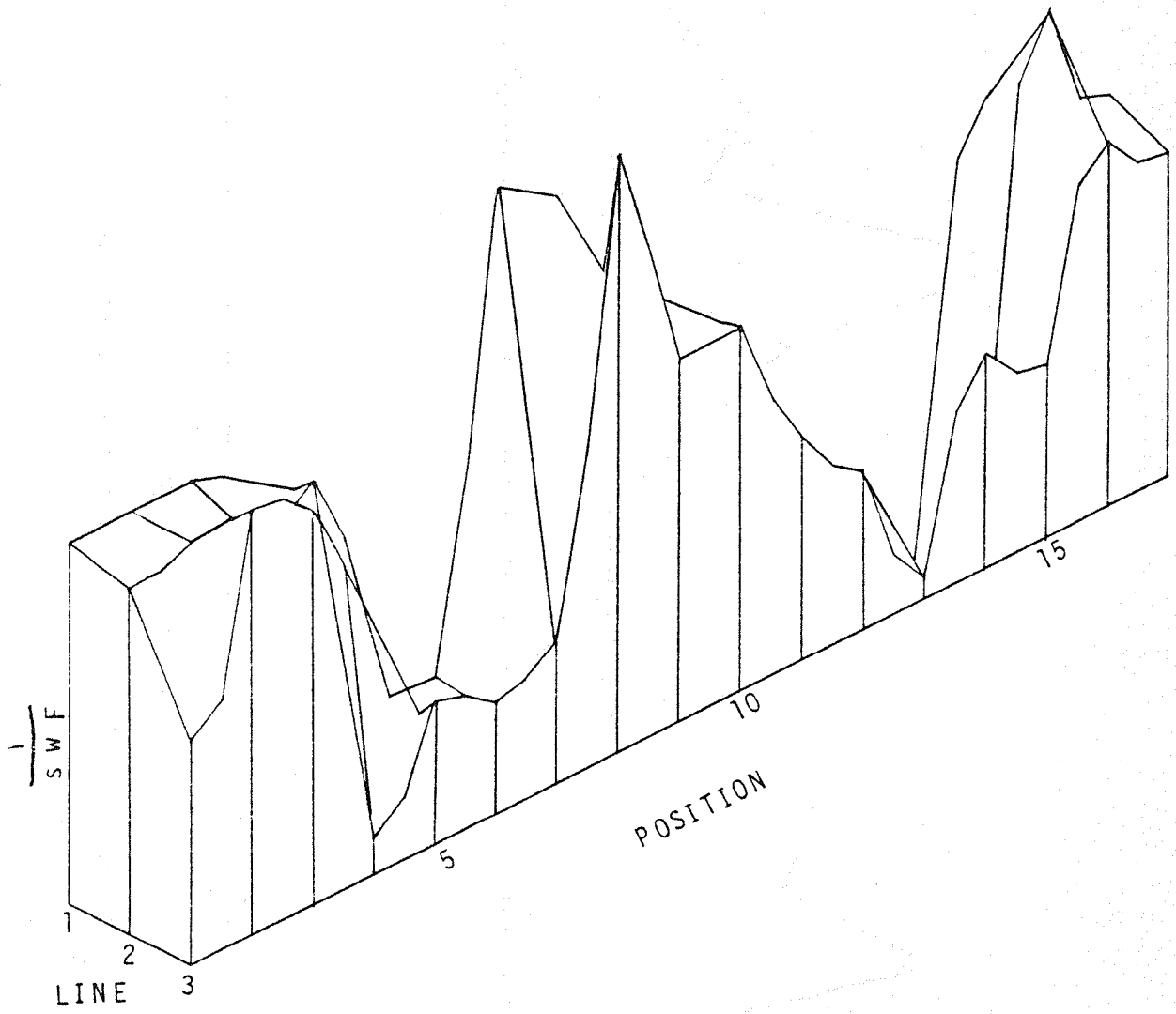


Figure 6. - 3-D plot of the SWF versus location on specimen.

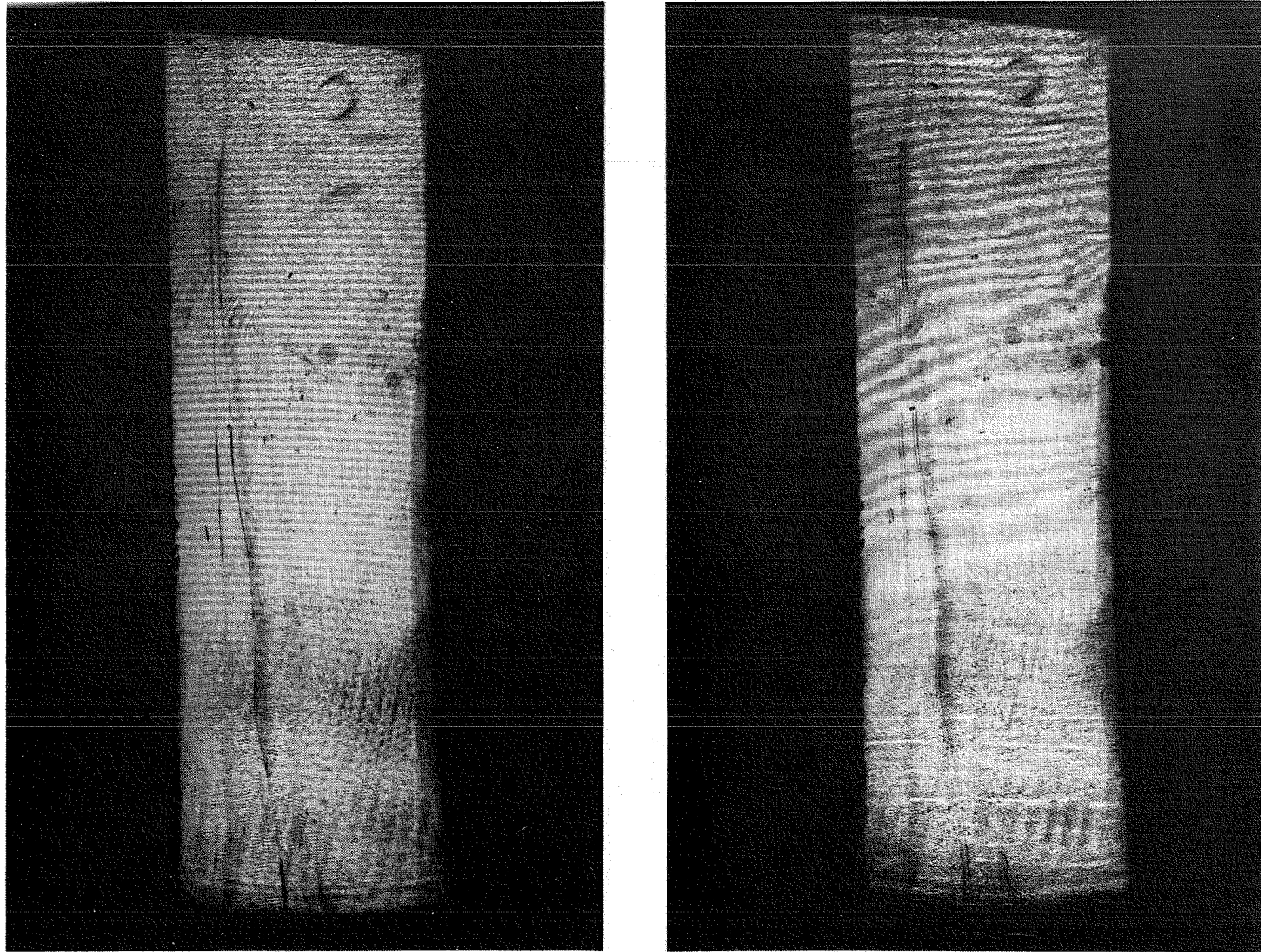


Fig. 7. - Moiré fringe patterns at (a) 500  $\mu\epsilon$  showing uniform  $u$  displacement field, and (b) 1800  $\mu\epsilon$  showing nonuniform  $u$  displacement field.

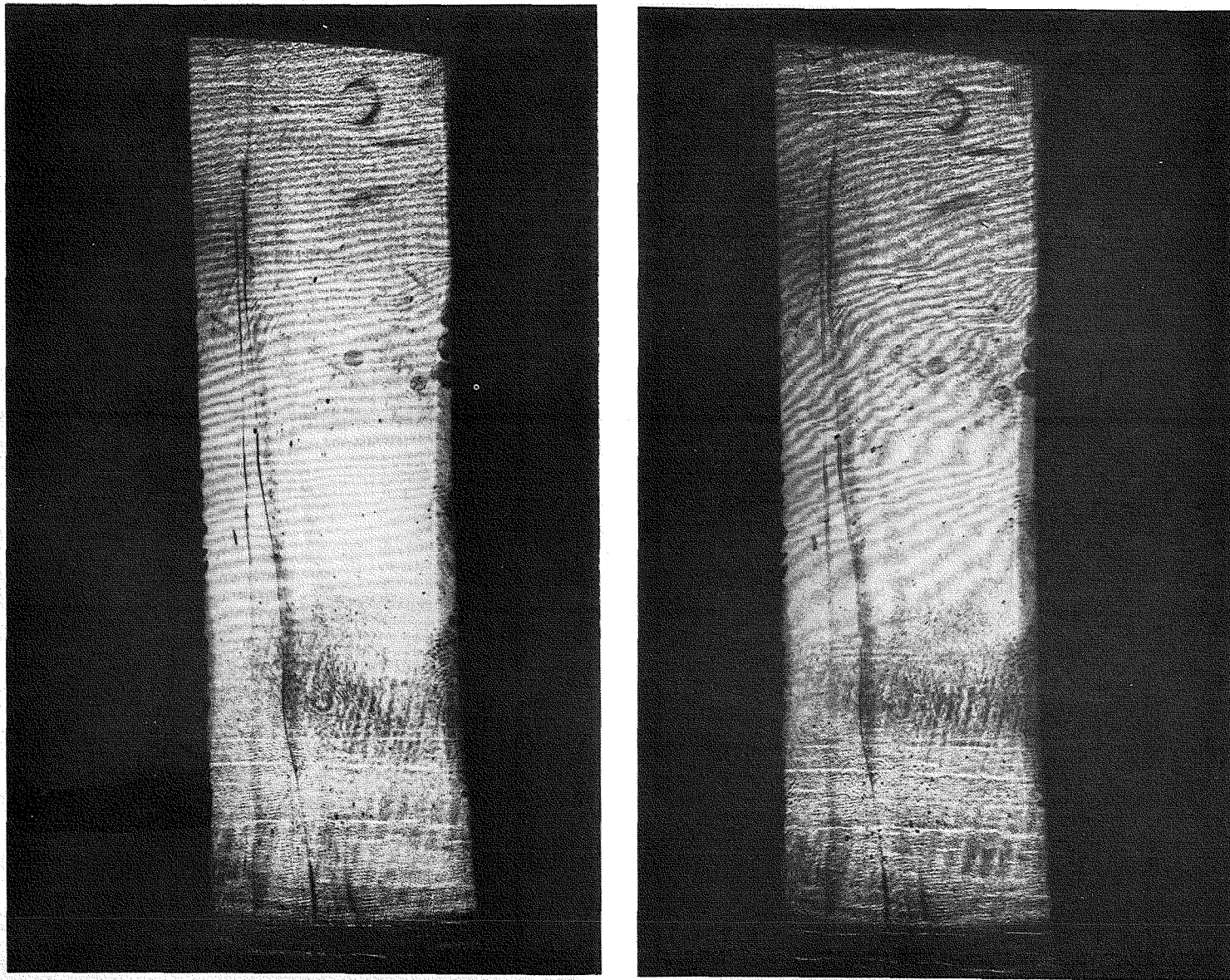


Fig. 8. - Moiré patterns at (a) 2000  $\mu\epsilon$ , before the first ply failure in  $(0,90_3)_S$  E-glass epoxy laminate, and (b) 2300  $\mu\epsilon$  after the first ply failed.

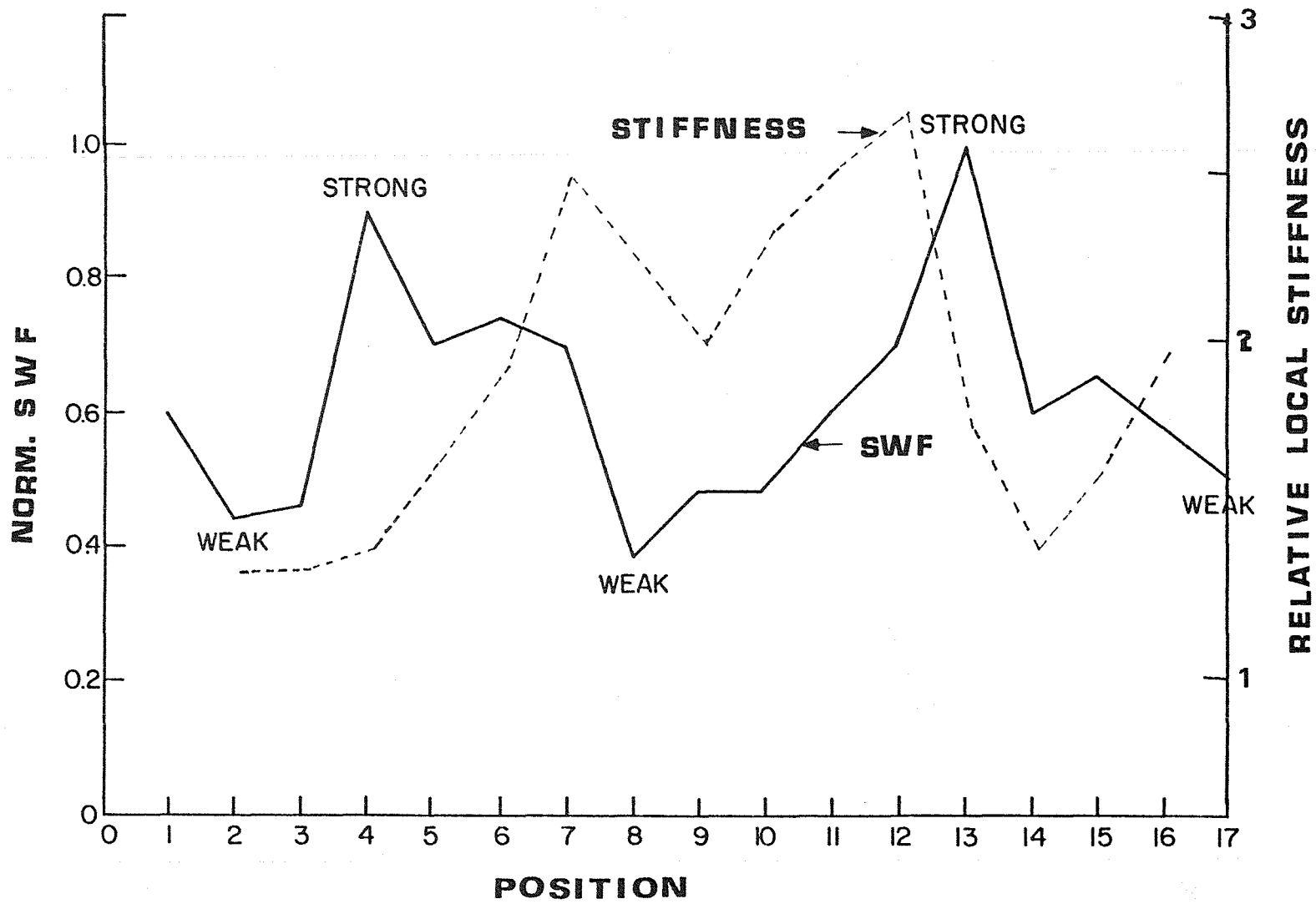


Figure 9. - Plot comparing average (normalized) SWF and local stiffness vs. position on specimen.

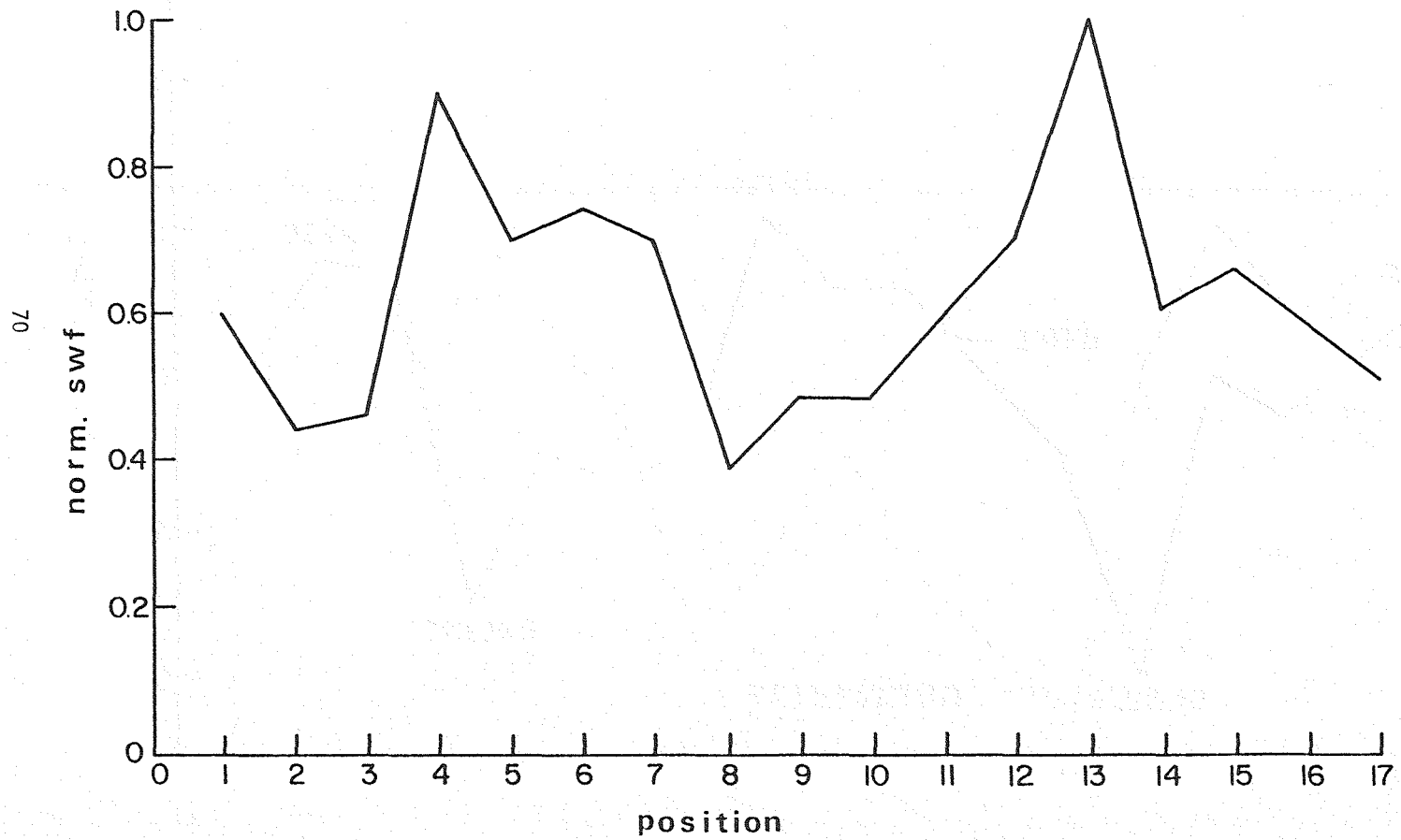
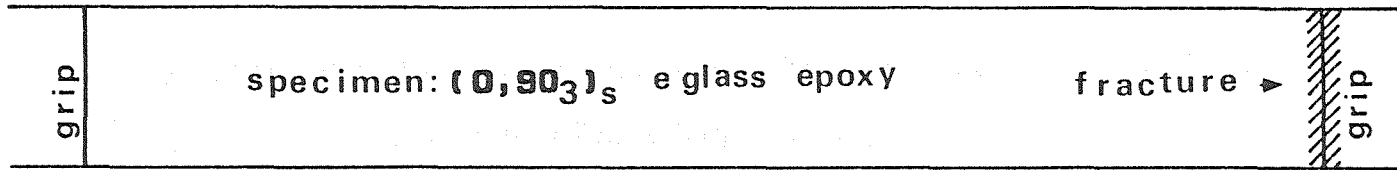


Figure 10. - Fracture location on specimen relative to SWF plot.

1. Report No. NASA CR-3670	2. Government Accession No.	3. Recipient's Catalog No.	
4. Title and Subtitle <b>A STUDY OF THE STRESS WAVE FACTOR TECHNIQUE FOR THE CHARACTERIZATION OF COMPOSITE MATERIALS</b>		5. Report Date February 1983	
		6. Performing Organization Code	
7. Author(s) Edmund G. Henneke II, John C. Duke, Jr., Wayne W. Stinchcomb, Anil Govada, and Alan Lemascon		8. Performing Organization Report No. None	
		10. Work Unit No.	
9. Performing Organization Name and Address Virginia Polytechnic Institute and State University Engineering Science and Mechanics Department Blacksburg, Virginia 24061-4899		11. Contract or Grant No. NSG-3-172	
		13. Type of Report and Period Covered Contractor Report	
12. Sponsoring Agency Name and Address National Aeronautics and Space Administration Washington, D. C. 20546		14. Sponsoring Agency Code 505-36-22 (E-1495)	
		15. Supplementary Notes Final report. Project Manager, Alex Vary, Materials Division, NASA Lewis Research Center, Cleveland, Ohio 44135. Appendix - Correlation of the Stress Wave Factor with Moiré Interferometry by Anil Govada.	
16. Abstract A testing program has been undertaken to provide an independent investigation and evaluation of the stress wave factor technique for characterizing the mechanical behavior of composite laminates. The present report details some of the data which have been obtained after performing a very large number of tests to determine the reproducibility of the SWF measurement. It has been determined that, with some optimizing of experimental parameters, one can reproduce the SWF value to within $\pm 10\%$ . Results are also given which show that, after careful calibration procedures, the lowest SWF value along the length of a specimen will correlate very closely to the site of final failure when the specimen is loaded in tension. Finally, using a moiré interferometry technique, it was found that local regions having the highest in-plane strains under tensile loading also had the lowest SWF values.			
17. Key Words (Suggested by Author(s)) Nondestructive testing; Ultrasonics; Acoustics; Interferometry; Composites; Strength; Fracture; Stiffness; Stress waves		18. Distribution Statement Unclassified - unlimited STAR Category 38	
19. Security Classif. (of this report) Unclassified	20. Security Classif. (of this page) Unclassified	21. No. of Pages 72	22. Price* A04

**End of Document**